

UNIVERSITY OF TWENTE.

Faculty of Electrical Engineering,
Mathematics & Computer Science

Embedded wearable device for monitoring diabetic foot ulcer parameters

Vishwajit V. Kulkarni
Thesis Report
November 2019

Supervisors:
dr. N. Meratnia
prof.dr. P.J.M. Havinga
dr.ir. A.B.J. Kokkeler

Faculty of Electrical Engineering,
Mathematics and Computer Science
University of Twente
P.O. Box 217
7500 AE Enschede
The Netherlands

Abstract

Diabetic foot complication is one of the leading cause of non-traumatic lower extremity amputations. Due to diabetic complications such as neuropathy, diabetic patients do not feel any pain in their feet. Due to this they are often unaware of any ulcer or wound formed on their feet. This along with impaired healing of the wounds often escalates into lower extremity amputation affecting patient's socio-economic well-being.

This graduation assignment aims to avoid occurrence of diabetic foot ulcers by monitoring different parameters of the foot and using it for predicting possible occurrence of ulcer. Developing and then evaluating hardware and software for this purpose comes under the scope of this master assignment. Designing such a system will help in taking early preventive measures for the feet to avoid occurrence of ulcer thereby avoiding further complications.

Acknowledgements

This master thesis would not been possible without the collective effort put by the people around me and I take this opportunity to acknowledge their contribution.

First and foremost, I would like to thank my supervisor dr. Nirvana Meratnia for her suggestions, support and direction throughout the thesis process. Without her guidance this thesis would not been in such a wonderful state as it is now. I would also like to thank my committee members prof.dr. Paul Havinga and dr.ir. Andre Kokkeler. When at a crossroad, their valuable advice and guidance helped me to analyse the problem from a different perspective.

I would like to thank the Pervasive Systems group members for their wonderful company that made my time during the thesis easier and truly memorable. I truly acknowledge and thank Rob and Fatjon for their support and valuable advice. I am also highly grateful to Nicole Baveld for providing me with all the possible facilities required for the successful completion of the project.

I would like to express my hearty gratitude to my parents for their unwavering faith in me and undying support that kept me strong emotionally through the entire journey of my graduate program. I take this opportunity to thank my friends : Husain, Zaid, Parth, Akash, Sharan, Nimish, Aniket, Sanlap, Ashwini, Navin, Shubham, Anusha, Lijun, Akshay, Harshad, Chinmayee, Rutuja, Saurabh, Aftab and Omkar. In Netherlands or back in India you guys always stood besides me throughout the journey. I can not put the feeling of gratitude in words.

Milind mama this thesis is dedicated to you.

Thank you so much!

Contents

List of Figures	ix
List of Tables	xiii
List of Acronyms	xv
1 Introduction	1
1.1 Diabetic Foot	1
1.2 Incidence and Implications	1
1.3 Problem Statement/Research Objective	1
1.4 Design Requirements	2
1.5 Thesis Outline	2
2 Brief Introduction to Diabetes and Diabetic Foot	5
2.1 Diabetes: Types and Causes (Pathophysiology)	5
2.2 Diabetic Foot	6
2.3 Why ulcers don't heal in diabetes?	9
2.4 Summary	10
3 Diabetic Foot Ulcer Indicators	11
3.1 Temperature	11
3.2 Pressure	12
3.3 pH	13
3.4 Summary	14
4 State of the Art	15
4.1 Commercial Systems	15
4.2 Relevant Work in Literature	15
4.3 Market research for socks	19
4.4 Summary	20
5 Hardware Design Exploration	21
5.1 Requirements	21
5.2 Choice of Sensors	21
5.3 Accelerometer Selection	25
5.4 Heart-Rate Monitoring	25
5.5 Sensor Conditioning and Calibration	26
5.6 Communication Protocol Selection	35
5.7 MCU selection	37

5.8 Summary	38
6 Software Design Exploration	41
6.1 Brief overview of Bluetooth Low Energy	41
6.2 CC2640 MCU Firmware	43
6.3 Android Application	46
6.4 Summary	48
7 System Integration	51
7.1 Sensor Placement	51
7.2 Sock Version 1.0	52
7.3 Sock Version 2.0	53
7.4 Technical Difficulties	54
7.5 Summary	54
8 Test and Evaluation	55
8.1 Sock Version 1 Test	55
8.2 Sock Version 2 Test	59
8.3 Shoe Evaluation	61
8.4 Power Profiling	62
8.5 Usability and washability	64
8.6 Summary	65
9 Conclusion	67
10 Future Work	71
Bibliography	72
A Complete test results : Thermistor calibration using conditioning circuit	77
B Datasheet: Temperature Sensor	79
C Complete pressure sensor readings for different postures	81
D Complete pressure readings for gait analysis	83

List of Figures

2.1	Role of α and β cells in blood glucose level control and its impairment in diabetes. Adopted from Bayenst et.al. (Baynest, 2015)	5
2.2	Classification of Diabetes Mellitus. Adopted from Association et al. (2013)	6
2.3	Different possible pathways for diabetic ulcer formation and amputation (adopted from (Frykberg et al., 2006)).	7
2.4	Example of callus formation under high pressure points. Adapted from (Alavi et al., 2014)	8
2.5	Illustration of Wound healing process in healthy individual. (adopted from (John Maynard, 2015))	9
3.1	Temperature difference between two legs one week before ulceration (adopted from (Armstrong et al., 2007)).	11
3.2	Relation between pressure, foot risk and foot deformity (adopted from Lavery et al. (2003))	12
3.3	a) Changes in pH milieu for acute wounds. b) Changes in pH milieu for chronic wounds. (adopted from (Ono et al., 2015))	13
4.1	Designs of three insole systems: (from left to right) Pedar, Medilogic and Tekscan. (Adopted from Price et al. (2016)	15
4.2	Examples of platform based pressure measurement systems.	16
4.3	WalkinSense pressure measurement system. (Healy et al. (2012))	16
4.4	Different pressure measurement systems in literature	17
4.5	Different foot measurement systems found in literature.	18
4.6	Different foot measurement systems found in literature.	19
5.1	An Example of working principle of optical force sensor. Any movement due to load (a-b) or shear force (c-d) affects the intensity of received light at the detector. (adopted from (Lincoln et al., 2012))	22
5.2	Basic construction of Shunt and Thru mode force sensing resistors. The resistance of pressure sensitive layer changes according to applied pressure. (Taken from Tekscan (2019))	23
5.3	Working principle of thermocouple. (adopted from (Jon Gabay, 2013))	24
5.4	Example of non-linear Resistance Vs Temperature characteristics of NTC thermistor.	25
5.5	Working principal of heart-rate sensor	26
5.6	Block diagram of pressure sensor calibration setup.	27
5.7	Plot of ADC Readings obtained for different pressure values exerted on the FSR.	28
5.8	FSR conditioning circuit for low/battery powered devices.	28
5.9	Calibration curve for FSR ADC Readings versus weight with $R_{\text{feedback}} = 50k\Omega$	29
5.10	Calibration curve for FSR ADC Readings versus weight with $R_{\text{feedback}} = 100k\Omega$	29

5.11	Block diagram of temperature sensor calibration setup	32
5.12	Test setup for temperature sensor calibration.	32
5.13	Temperature calibration curve for temperature sensor without conditioning circuit.	34
5.14	Temperature calibration curve for temperature sensor with conditioning circuit.	35
6.1	Bluetooth Low Energy Architecture. (Adopted from Mohammad Afaneh (2016))	41
6.2	GATT protocol organization.	43
6.3	Functional block diagram of CC2640. (Image source: Texas Instruments)	44
6.4	Execution flow of CC2640 firmware.	45
6.5	Selected code snippets of CC2640R2F firmware.	46
6.6	Abstract flow diagram of smart sock android application	47
6.7	Examples of Android application screens.	50
7.1	Different areas of the foot based on pressure distribution. (Adopted from (Shu et al., 2010))	51
7.2	Pressure sensor locations on the plantar side of the foot. Temperature sensors are placed at the same location from the inside.	51
7.3	Sensor breakout board designed for sensor conditioning and multiplexing.	53
7.4	Sock prototype version-1	53
7.5	Single board design for signal conditioning, MCU and RF circuitry operated on coin-cell battery	53
7.6	Sock prototype version-2. Note the use of conductive thread removes dangling wire connections from the sensor.	53
8.1	Variation in pressure readings at toe, MTH1 and heel for different postures. For all sensor readings refer Appendix C	55
8.2	Variation in accelerometer readings for X axis for different postures.	56
8.3	Different phases of gait cycle. (Adopted from (Mariani et al., 2013))	56
8.4	Pressure readings at toe, MTH1 and heel for gait cycle (53 steps each leg). For all sensor readings refer Appendix D	57
8.5	Accelerometer readings (x-direction) for gait cycle (53 steps each leg).	57
8.6	Temperature readings for different areas of the foot.	58
8.7	Temperature readings for different areas of the foot when foot is subjected to varying temperature using heat source.	58
8.8	Pressure readings of Toe, MTH1 and heel for different postures.	59
8.9	X-axis accelerometer readings for different postures.	59
8.10	Pressure readings for gait cycle (19 steps each leg).	60
8.11	Accelerometer readings (x-direction) for gait cycle (19 steps each leg).	60
8.12	Temperature readings for different areas of the foot.	61
8.13	Temperature readings for different areas of the foot when foot is subjected to varying temperature using heat source.	61

8.14 Different shoes (sport shoes and high-heel) used to evaluate their effectiveness in distribution of the foot pressure.	62
8.15 Pressure readings for sport shoes and high heels in standing position.	62
8.16 Test setup for power measurement. The Sock is connected as device under test (DUT).	62
8.17 Power profiler results for Bluetooth advertising.	63
8.18 Summary of usability test results	64

List of Tables

4.1	Comparison of three insole systems. (Adopted from Price et al. (2016))	15
5.1	FSR Readings for resistor divider network setup	27
5.2	FSR Readings with $R_{\text{feedback}} = 50k\Omega$	30
5.3	FSR Readings with $R_{\text{feedback}} = 100k\Omega$	30
5.4	Temperature sensor calibration without conditioning circuit.	33
5.5	Statistics of calibration test without conditioning circuit.	33
5.6	Selected test results for temperature sensor calibration using conditioning circuit. (For complete Table refer Appendix A).	34
5.7	Statistics of calibration test results using conditioning circuit.	35
5.8	Comparison of different wireless technologies. (Adopted from (Al-Sarawi et al., 2017; Patrick Mannion, 2017))	37
5.9	Comparison of different Bluetooth enabled microcontrollers	39
8.1	Usability survey results	64
A.1	Complete test results for temperature sensor calibration using conditioning circuit.	77

List of Acronyms

PVD	Peripheral Vascular Decease
DFU	Diabetic Foot Ulcer
DM	Diabetes Mellitus
FBG	Fiber Bragg Grating
RF	Radio Frequency
MCU	Micro-controller Unit
LED	Light Emitting Diode
FSR	Force Sensing Resistor
PCB	Printed Circuit Board
RTD	Resistor Temperature Detector
NTC	Negative Temperature Coefficient
IC	Integrated Circuit
ADC	Analog to Digital Converter
STD	Standard Deviation
Op-Amp	Operational Amplifier
ANT	Advanced and Adaptive Network Technology
WiFi	Wireless Fidelity
NFC	Near Field Communication
LE	Low Energy
BLE	Bluetooth Low Energy
SPI	Serial Peripheral Interface
I²C/ I2C	Inter Integrated Circuit
SDK	Software Development Kit
GPIO	General Purpose Inputs and Outputs
BR	Basic Rate
EDR	Extended Data Rate
GAP	Generic Access Protocol
GATT	Generic Attribute
GUI	Graphical User Interface
CCCD	Client Characteristic Descriptor

1 Introduction

Diabetes is one of the commonly known and found disease all around the world with no permanent cure found yet. It is estimated that by 2025 more than 65 million people in Europe will suffer from diabetes (Lepäntalo et al., 2011) whereas global estimation is around 300 million (Zimmet et al., 2001). Diabetic foot is condition caused due to effects of diabetes and often leads to amputations and in some cases even to death. Hence, it is important to detect diabetic foot condition at an early stage to avoid the foot complications.

1.1 Diabetic Foot

Diabetic foot is an umbrella term used to describe medical condition such as ulcer, ischemia, infection or other complications of the lower limb caused due to diabetes and its effects. The most common problem found in diabetic foot is advanced ulceration of the foot which often requires surgical intervention and in many cases amputation. The cause of this problem can be narrowed down to three conditions: neuropathy, impaired healing and peripheral vascular disease (PVD).

Neuropathy adversely affects the ability to sense pain, causing diabetic patients to become completely unaware of the damage caused to the foot. In addition to this, wound healing is slowed down or even stalled due to the effects of diabetes. In some cases, patients also suffer from peripheral vascular disease which affects blood supply available to the lower extremities of the body. These three combined conditions lead to situations where patient realises the damage done to foot very late, resulting loosing part of their lower limb.

1.2 Incidence and Implications

Incidence of Diabetic Foot Ulceration (DFU) around the world is very common and is major cause of amputations. Around 85% of amputations in diabetic conditions are caused due to diabetic foot ulcer. About 46% of hospitalization cases for foot ulcer in US are from diabetic condition which comprises only 4% of the overall population (Reiber et al., 1998). Moreover, every 30 seconds someone loses their lower limb as an effect of diabetic foot complication (Boulton et al., 2005).

This adversely affects both social and economic conditions of the individual. The costs incurred due to diabetic foot depend on several factors such as medication costs, surgical interventions, footwear and in-patient costs. In study by Boulton et al., authors claim that around 20% of all the expenditure on diabetes is spent on diabetic feet. This expenditure ranges from US \$993 to US \$17519 (1998 equivalent) depending on the severity Boulton et al. (2005). Survival rates after amputation do not paint an optimistic picture either. Perioperative mortality rates after amputations are 9% in Netherlands where as survival rate 3 years after amputation are just 59% in Sweden and 50% in Italy (Jeffcoate and Harding, 2003).

1.3 Problem Statement/Research Objective

All of this data points towards importance of detecting ulceration at the early stages. If the occurrence of ulceration is prevented, then it will altogether eliminate conditions that follow it, preventing the social and financial burden it carries. There have been substantial amount of research done around this problem. There are studies which focus on pressure, defining limits for safe and unsafe pressure values, temperature and its relevance to ulceration sites and so on. Based on these studies, there are applications which try to monitor these parameters to determine ulceration prone areas. However these studies mostly monitor these parameters using pressure mats or custom made footwear. These designs put limitations on amount of

time the foot parameters can be monitored. Also, patients are more aware of these recordings as they have to wear specific set of shoes or walk bare-feet on specific mat. Being aware of these reading can also result in false readings as patients try to compensate their gait due to their awareness.

This assignments tries to address these problems by trying to answer the following question: *To what extent, is it possible to continuously monitor foot ulcer indicators in an efficient, accurate, and user- friendly manner through embedding sensing and communication technologies in daily worn socks?*

This is achieved by finding solutions for following set of questions:

- *Which foot parameters can be used to predict incidence of DFU?*
- *What are functional and non-functional requirements of monitoring these parameters using a smart sock?*
- *What are the software and hardware requirements and design decisions for continuous monitoring and detection of foot ulcer using a smart sock?*
- *How accurately and efficiently the designed smart sock can measure the foot ulcer indicators?*
- *How user-friendly and comfortable is the designed smart sock?*

1.4 Design Requirements

Functional Requirements

1. The developed sock should be able to monitor required foot parameters continuously.
2. Sock should be designed to be worn in day to day life. Design should be clean and should not affect or change the normal bio-mechanics of the foot causing errors in the readings.
3. Sensors data must be reproducible and repeatable
4. Sufficient battery life must be ensured to take continuous readings for long duration.
5. Errors in sensor readings must be within specified limits.
6. System should be able to perform data logging.

Non-functional Requirements

1. *Safety*: The sock is designed for patients with neuropathy, which means they have very little or no sensation of pain. Thus it should be made sure that, the sock is not causing any damage to the foot skin while attempting to measure the same.
2. *Weight*: Weight of the sock should not cause any effect on walking or foot health.
3. Sock design should be size independent.
4. Sock should be washable and reusable within certain restrictions.

1.5 Thesis Outline

The organisation of this thesis is done as follows:

Chapter 2 provides the background information necessary to understand the types and causes of diabetes. Subsequently, the underlying causes behind diabetic foot are explained. The chapter finally concludes with discussion of the complications of wound

healing in diabetic patients. Thus, providing the motivation behind early detection of diabetic foot ulcer.

Chapter 3 presents the different indicators for detection of diabetic foot ulcer viz. temperature, pressure and pH. The literature where these parameters have been used for diabetic foot ulcer detection is examined and a decision of choice of parameters is presented and discussed.

Chapter 4 lists the existing commercial systems such as In-shoe systems, platform systems and sock systems which address the diabetic foot ulcer detection problem. A industrial survey focused only on socks is also presented along with motivation for selecting a smart sock design.

Chapter 5 presents the design space exploration performed for selecting different hardware components for the sock. The different sensors available for measurement of pressure and temperature are discussed and compared. The motivation behind choosing a certain type of sensor for pressure and temperature is presented. Additionally, the design decision for choosing accelerometer is discussed and heart-rate monitoring process is examined. Following this, the sensor calibration and conditioning performed for the pressure and temperature sensors is presented. The chapter concludes with the discussion of design choices behind selection of communication protocol and the microcontroller unit.

Chapter 6 provides the information about the design decisions taken during software design of the smart sock. The chapter begins with providing the background information about bluetooth low energy. This is followed by in-depth discussion of the design of Bluetooth firmware running on CC2640R2F Bluetooth MCU and Android application that compliments hardware design of the smart sock.

Chapter 7 provides the design details for two versions of the smart sock design. Initially, the motivation behind the chosen sensor placement arrangement is presented along with the accelerometer placement. This is followed by a discussion of the complete setup of the two sock designs. Finally, the various technical difficulties faced during sock developed are presented.

Chapter 8 is focused on the results obtained after evaluating the 2 sock versions when subject to different tests (pressure test, accelerometer test and temperature test). This is followed by evaluation of different shoes using the developed smart sock. The results obtain after power profiling the smart sock are presented. The chapter concludes with discussion of washability and usability tests performed on the sock.

Chapter 9 presents the conclusion for this research work where the main research question and sub questions formulated in Chapter 1 are addressed and answered.

Finally, Chapter 10 describes the future work possible in this research work.

2 Brief Introduction to Diabetes and Diabetic Foot

When we normally use the term 'Diabetes', we refer to Diabetes Mellitus (DM) since it is more prevalent than other type (Diabetes Insipidus). Although diabetes in itself is not a life-threatening disease, its long term effects can be severe. There is no cure found for yet. This means best what patients can do is to manage their blood sugar levels and keep it within bounds. This exposes them to risk of encountering diabetic complication throughout their life. Therefore, it is rudimentary that we should understand the way diabetes affects our body.

This chapter provides brief information about types and causes of diabetes, followed by diabetic foot condition and reasons of disrupted wound healing process in diabetic patients.

2.1 Diabetes: Types and Causes (Pathophysiology)

Blood sugar (glucose) level in our body is controlled by pancreas. Pancreas is responsible for secreting two hormones called insulin and glucagon which collectively control the sugar level in the blood. When blood sugar level is high, insulin is released in blood which directs cells to absorb and store the excess blood sugar in form of glycogen. When sugar level is low, glucagon hormone is released which directs cells to convert back glycogen into its original form (glucose) and release it in blood. The α and β cells present in pancreas are responsible for maintaining the sugar levels at normal value. Figure 2.1 shows the blood glucose control mechanism for normal and diabetic conditions.

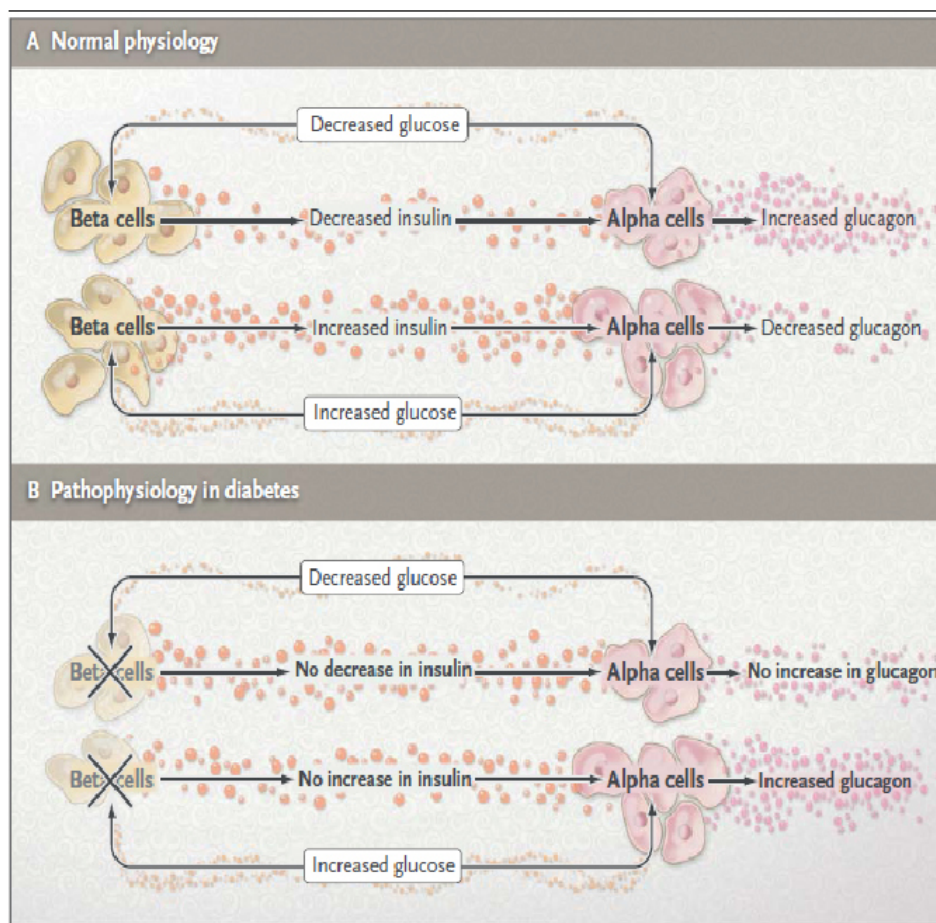


Figure 2.1: Role of α and β cells in blood glucose level control and its impairment in diabetes. Adopted from Bayenst et.al. (Bayenst, 2015)

2.3 illustrates different pathways leading to diabetic foot ulceration. This section provides brief introduction to these pathways for better understanding of underlying causes of the diabetic foot ulceration.

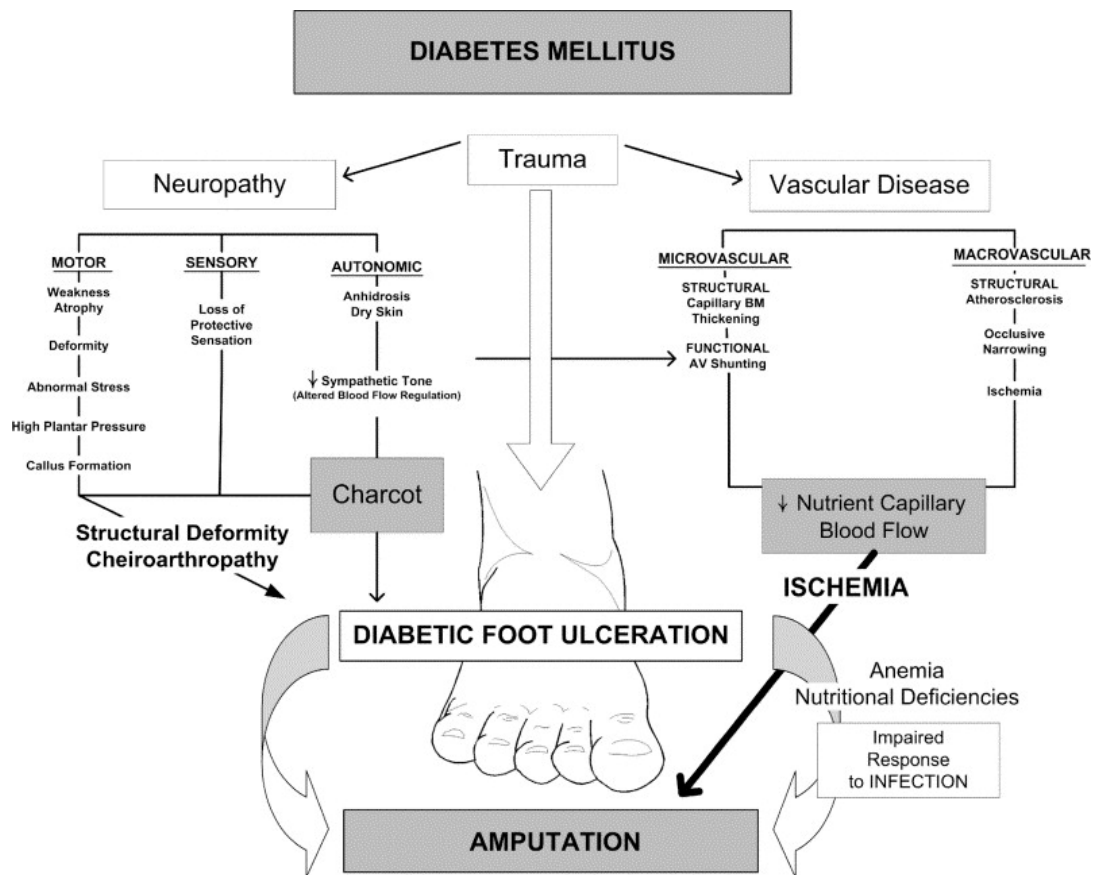


Figure 2.3: Different possible pathways for diabetic ulcer formation and amputation (adopted from (Frykberg et al., 2006)).

2.2.1 Neuropathy

Neuropathy affects the sensation of pain experienced by diabetic patients and also disrupts temperature discrimination and automatic functions. Due to reduced sensibility of sensory systems to stimulus such as touch, temperature and vibrations, patients become unaware of early signs of foot ulcers as well as foot deformity (Ahmad, 2016). In most of the cases longest motor fibers are affected first. This results into damage of sensory and motor functions of lower leg and hands, called as stocking and glove distribution (Bandyk, 2018). Motor neuropathy alters bio-mechanics and foot anatomy causing limited joint mobility and altered loading of the foot (Lepántalo et al., 2011). Dislocation of tarsal bones produces a bowed, “rocker-bottom” appearance of the foot which is susceptible to high pressure ulceration.

2.2.2 Peripheral Vascular Disease (PVD)

Blood supply to the foot is provided by three blood vessels : posterior tibial artery, anterior tibial artery and peroneal artery. Diabetes can affect one or more of these arteries. For every 1% increase in $HbA1c$ ¹, there is corresponding 25-28% increased risk of PVD (Selvin et al., 2004). Patients with diabetes frequently develop micro-arterial dysfunction that begins early in life which limits capillary blood capacity. This loss of capillary capacity reduces body’s ability

¹The hemoglobin A1c ($HbA1c$) test provides average level of blood sugar over past 2 to 3 months. It’s also called glycated hemoglobin test and glycohemoglobin.



Figure 2.4: Example of callus formation under high pressure points. Adapted from (Alavi et al., 2014)

to provide oxygen and other nutrients to tissue and hence healing and restoration of tissue is impaired. This can also result in ischemia or neuro-ischemia (in presence of neuropathy) which renders foot more susceptible to ulcer formation. In general skin perfusion can be used as an indicator of good lower extremity microcirculation (Alavi et al., 2014).

2.2.3 Charcot Foot

The Charcot foot presents itself as a late complication of peripheral motor neuropathy. DM is the most common cause of Charcot deformity in the Western world and should be considered in any patient who presents a warm swollen foot, with or without ulceration (Alavi et al., 2014). Due to absence of pain as result of sensory neuropathy, continuous weight bearing may lead to destruction and distortion of the joints (Levy and Valabhji, 2008). This dislocation and distortion of joints without any significant trauma are characteristics of Charcot foot. It might present symptoms such as deformity, swelling, increased foot temperature and redness. Charcot foot results in rocker bottom deformity which makes foot prone to ulceration due to uneven weight distribution.

2.2.4 Infection

Infection generally does not present itself as a cause of foot ulcer, however, presence of neuropathy and PVD makes foot susceptible for infections. In the presence of damaged or poorly perfused skin and soft tissues, rapid bacteria penetration going deep to fascia can occur, producing a foot-threatening infection and sepsis (Bandyk, 2018). These deep infections are manifested either as osteomyelitis² or a soft tissue infection spreading along the tendons in the compromised foot (Lepäntalo et al., 2011). Such deep infection results in immediate requirement of amputation in 25-50% of cases. In chronic wounds, microorganisms aggregate together and grow within communities where they encase themselves within extracellular polymeric substances (Alavi et al., 2014). Such encased microorganism communities are called as biofilms and exhibit resistance to chemical, antimicrobial and immunological measurements. This increases complications as antimicrobial medications are ineffective in penetrating the biofilms and disinfecting the wound sites causing further delay in healing. Such cases require surgical intervention increasing cost and complexity of the treatment.

²Osteomyelitis is infection of the bone

2.3 Why ulcers don't heal in diabetes?

Wound healing in a healthy individual is a complex biological process involving well orchestrated integration of processes such as cell migration, cell proliferation and extracellular matrix deposition (ECM) (Falanga, 2005). In addition to the factor of health condition, degree of injury and certain diseases can affect rate of healing. Normal wound healing can be broadly divided into four phases namely coagulation, inflammation, proliferation and remodelling as shown in Figure 2.5. These phases are not distinct and often overlap throughout the healing process.

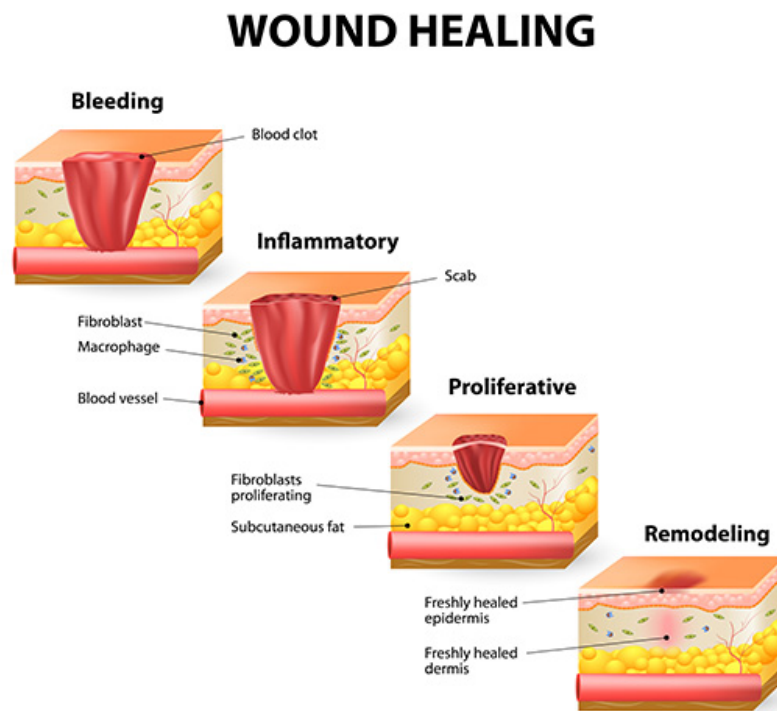


Figure 2.5: Illustration of Wound healing process in healthy individual. (adopted from (John Maynard, 2015))

However clinical and experimental evidence suggests that diabetic ulcer does not follow normal healing order and certain stages get prolonged or become stagnant. Effects of diabetes like neuropathy and poor blood circulation are the causes of this impaired healing process.

These conditions affect wound healing in following ways:

- **POOR CIRCULATION**

High blood sugar (glucose) levels alters the thickness or consistency of the blood. Because of this blood vessels get affected and become more stiff as well as narrow thereby reducing extent of blood-circulation (perfusion) to the cells. This results in condition where cell present in wound area do not get required supply of oxygen and other nutrients which are essential for healing process.

- **NEUROPATHY**

Neuropathy affects joint mobility and deprives patients from the ability to sense pain at the limb extremities. Because of this, patients are often unaware of the existence of wound which delays the time of preventive medications and bandages. In addition to this, limited joint mobility and uneven foot pressure distribution worsens the damage level of the wound site and can also lead to new ulcer formation.

- IMMUNE SYSTEM DEFICIENCY

Diabetic patients can suffer from immune system deficiency as cause or effect of diabetes. Such condition affects number of immune cells and their ability to take preventive actions against foreign elements.

2.4 Summary

Diabetes is a disease with no cure and affects our body function in different ways. These long term effects such as neuropathy and PVD often lead to situation where patients are unaware of the changes in anatomy and have lost sensation of the pain exposing them to risk of ulceration. However, there are few indicators found in literature that can help in predicting high risk ulceration sites. Next chapter delves into these indicators and how they can be used to predict ulcers.

3 Diabetic Foot Ulcer Indicators

In this chapter, we will look at different foot parameters which can be used to predict diabetic foot ulcer episode. An investigation into current literature points towards three parameters than can be used to ulcer prediction. These parameters are : temperature, pressure and pH. These parameters are analysed and discussed on the basis of evidence found in literature.

3.1 Temperature

For non-invasive remote monitoring of diabetic foot, temperature measurements can be used as a base parameter. Human skin plays a pivotal role in thermo-regulation of the body. Temperature of human body is the result of thermal balance between thermal energy supplied by core and energy lost to the environment via conduction, convection, radiation and evaporation (Fierheller and Sibbald, 2010). Studies of dermal thermometry have suggested that variations in temperature $> 4^{\circ}F$ ($> 2.2^{\circ}C$) could be helpful in skin surveillance (Armstrong et al., 2007). This rise in temperature can be detected up to one week before actual foot ulceration occurs (Liu et al., 2013). However there is no reference range available as body temperature can vary widely from person to person and even within different body parts of the same individual.

This difficulty can be overcome by comparing one part of the body with its symmetrical counter part since under normal circumstances they are considered to be comparable (Fierheller and Sibbald, 2010; Jones, 1998). Clinical studies on the home monitoring of plantar foot temperature have shown that frequent temperature assessment, and, treatment in the case of temperature differences greater than $2.2^{\circ}C$ between same regions of both foot, can prevent diabetic foot complications (Liu et al., 2015). In the studies performed by Armstrong et al. (2007), authors found that, temperature difference between ulcerated foot regions was 4.8 times higher than that of region without ulceration. This difference depicted in Figure 3.1 was found almost a week prior to ulceration.

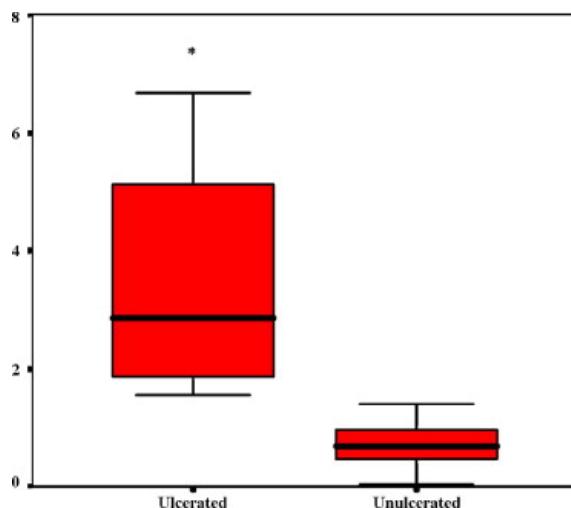


Figure 3.1: Temperature difference between two legs one week before ulceration (adopted from (Armstrong et al., 2007)).

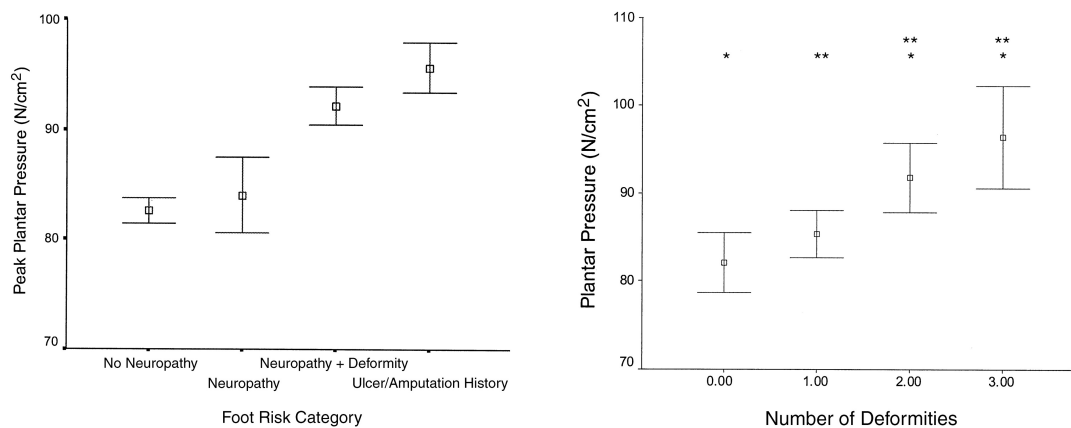
Skin temperature is relatively easy to measure and few studies have taken advantage of this by letting patients keep log of their foot temperature as part of self-check. One such study performed by Lavery et al. (2007) highlighted positive impact of temperature measurements. The study was performed on the controlled group of 173 individuals divided into three groups. The group that was directed to measure temperature and report if difference in temperature

is more than 2°C displayed only 8.5% risk as compared to $\approx 30\%$ risk in other groups. These findings strongly support use of temperature for diabetic ulcer prediction.

3.2 Pressure

Diabetic foot ulcers mostly manifest as combined effect of neuropathy, peripheral vascular disease, bone and tissue deformity which results in repetitive pressure on certain areas of the feet. Hence, inclusion of pressure sensors in a device for diabetic ulcer prediction is an intuitive choice. There is significant literature available that looks into the increased foot pressure and its correlation with ulcer formation. In a paper presented by Duckworth et al. (1985), authors inspected the pressure measurements using static and dynamic measurement techniques. Static techniques measure pressure when person is standing still where as dynamic measurements are done when person is moving (e.g. walking). It is well established that abnormally high pressure points are common with severe neuropathic conditions or in patients with prior ulcer history (Duckworth et al., 1985) and this is supported by numerous studies found in the literature (Lavery et al., 2003; Caselli et al., 2002; Bernard et al., 2009; dos Reis et al., 2010).

Lavery et al. (2003) assessed a cohort of 1666 patients to measure effectiveness of plantar foot pressure in predicting patients with high risk of ulceration. The findings of their study are depicted in Figure 3.2. This study effectively shows that persistent high pressure areas of the foot directly relate with high risk of ulceration. Their study showed that elevated pressure doubles risk of ulceration. Generally pressure greater than 6 kg/cm^2 is considered as high pressure site with risk of ulceration. However different studies use different value as threshold. In addition to this difference of measurement setups, methods and units makes choosing universal threshold difficult.



(a) Peak pressure with respect to foot risk category. Increasing foot risk is directly reflected in increase of plantar foot pressure.

(b) Effect of forefoot deformity on plantar pressure. It can be seen that increased number of deformities strongly co-relates with increased plantar pressure.

Figure 3.2: Relation between pressure, foot risk and foot deformity (adopted from Lavery et al. (2003))

Caselli et al. (2002) overcome this issue by taking ratio of forefoot to rear-foot pressure (F/R) of the same foot. This approach offers some advantages: since it is a ratio, it is absolute value that is independent of measurement unit. Also since both pressure measurements are taken from the same foot, external factors involved are common making it fairly independent of external factors. Their study has shown that F/R value of 2 or more can predict ulceration risk with the same specificity as a peak pressure of 6 kg/cm^2 .

Waaajman et al. (2014) measured pressure inside the shoe along with bare feet pressure measurements. This was done due to fact that bio-mechanics of the foot changes when footwear is put on. The pressure at foot-insole interface will be modified because of shape and material

of the insole (Duckworth et al., 1985). For such footwear, it must be made sure that in-shoe peak plantar pressure is kept less than 200 kPa (Waaaijman et al., 2014). Such measurements can also get affected due to the errors induced due to conscious or unconscious off-loading of foot by subjects due to awareness about the test (Duckworth et al., 1985) and such factors must be taken into account while designing the footwear.

These various studies point towards use of pressure changes and abnormal pressure values recorded from different region of the foot as a ulceration risk factor, Hence pressure can be used as primary indicator for possible ulceration.

3.3 pH

Human skin acts as a barrier between internal body environment and external micro-organisms and environmental changes. The normal value of pH of skin in healthy adults and children is slightly acidic and ranges between 4.2 - 5.6 (Ono et al., 2015). In contrast to this, body's internal environment maintains near neutral pH. This difference creates sharp gradient of about 2-3 pH units between skin surface and underlying epidermis and dermis (Ali and Yosipovitch, 2013). However there is not enough literature found which uses pH as indicator for DFU. Ali and Yosipovitch (2013) remark in their paper that 'In spite of mounting evidence that skin pH plays vital role in skin function, application of acid mantle concept in clinical care has lagged behind'.

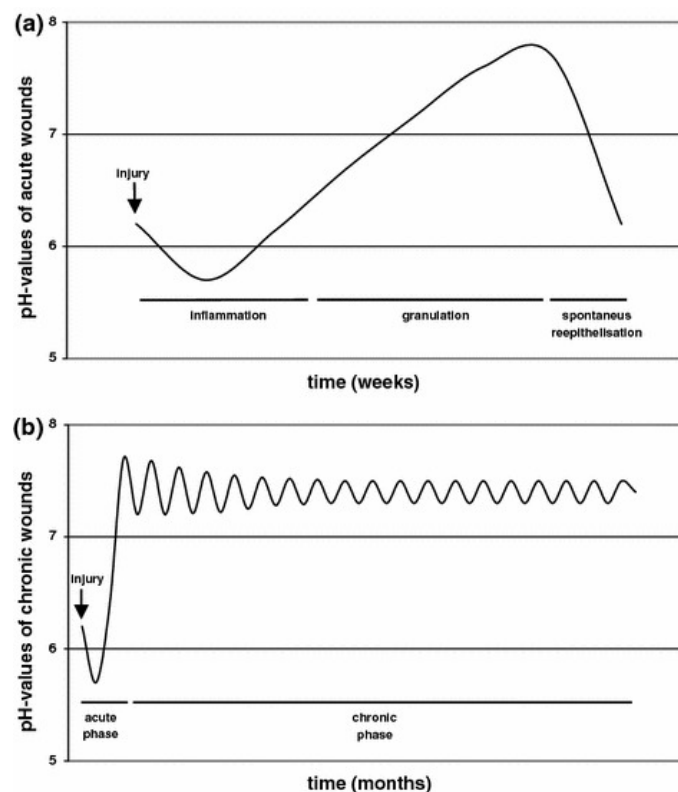


Figure 3.3: a) Changes in pH milieu for acute wounds. b) Changes in pH milieu for chronic wounds. (adopted from (Ono et al., 2015))

There is some literature available which focuses on detecting change in pH values of the wound which indicate presence of infection. Healing wound goes to different phases and each phase shows different value of pH as shown in Figure 3.3. Nominal value of healing wound is within range of 5.5 - 6.5 (Mostafalu et al., 2018) whereas infectious wounds show pH values typically greater than 9. This difference is used to design smart bandages which release drug based on pH reading as demonstrated in (Mostafalu et al., 2018).

Lack of sufficient literature does not encourage using pH as primary indicator for ulceration. Moreover use of soap, shower gel and even tap water can affect skin pH significantly (Lambers et al., 2006). But pH measurement can be used as secondary parameter along with temperature and pressure to aid detecting ulceration.

3.4 Summary

- The literature found about diabetic ulcer indicators strongly advocate use of pressure and temperature as primary indicators for ulceration.
- Persistent temperature changes can be observed since one week before ulceration.
- Both static and dynamic pressure can be used to measure pressure distribution of the foot under different conditions.
- Forefoot to rearfoot ratio (F/R) can also be used to predict ulceration.
- Use of pH change as indicator of ulceration lacks sufficient support by literature to be considered as primary indicator. However it can be used as secondary parameter or additional information to gain better insights.

Next chapter presents brief overview about the different wearbales designed for diabetic ulcer prediction using these parameters.

4 State of the Art

Last chapter looked into different foot parameters that can be monitored for prediction of diabetic foot ulcer. This chapter presents a short review of literature as well as commercial products based on the utilization of these parameters.

4.1 Commercial Systems



Figure 4.1: Designs of three insole systems: (from left to right) Pedar, Medilogic and Tekscan. (Adopted from Price et al. (2016))

Although there are several parameters available for prediction of diabetic ulcer, majority of commercial systems focuses on pressure measurement. Price et al. (2016) present comparison and evaluation of three commercial insole systems available in the market. These insole systems are shown in Figure 4.1. Table 4.1 summarises comparison between these three systems based on different features.

Feature	Pedar	Medilogic	Tekscan
Sensor model	Pedar-X	SohleFlex Sport	F Scan 3000E Sport
System cost (current quote)	£12,600	£10,500	£14,000
Sensor technology	Capacitive	Resistive	Resistive
Sensor density	0.57–0.78 per cm^2	0.79 per cm^2	3.9 per cm^2
Maximum sampling rate	100 Hz	300 Hz	169 Hz
Measurement range	20–600 kPa	6–640 kPa	345–862 kPa
Insole thickness (at sensor region)	2.2 mm	1.6 mm	0.2 mm

Table 4.1: Comparison of three insole systems. (Adopted from Price et al. (2016))

It can be seen that cost for all three of the insoles are very high. The reason for this high cost is due to high sensor density, high sampling frequency and comprehensive software provided for analysis. However such systems are focused on research and lab use. Home monitoring has less restrains in terms of all the features provided in the table such as sensor density and sampling rate but the cost of the system must be reasonable. Nevertheless these commercial systems are accurate and are used in many studies as reference for performance comparison.

4.2 Relevant Work in Literature

Similar to commercial systems, most of the literature is targeted towards pressure measurement. These literature refer to platform systems as standard measurement devices used in laboratories. This section first provides brief information about such platform systems followed by review of different in-shoe systems.

Platform Systems

Platform systems offer simple measuring systems that in which sensors are arranged in matrix format on flat surface. Most of the platform systems focus on pressure measurements. These surfaces can be rigid, flexible like mat or fixed into the flooring. Such set-ups are only suitable in research laboratories and rigorous tests across different surfaces reflecting real life scenarios are difficult to conduct (Tan et al., 2015). Since this is a special set up, patient needs time to familiarize with the setup to reproduce the natural gait. Also these systems are bulky and usage is restricted to non continuous indoor measurements. Figure 4.2 shows two example pressure measurement system by Zebris Medical and Novel respectively.

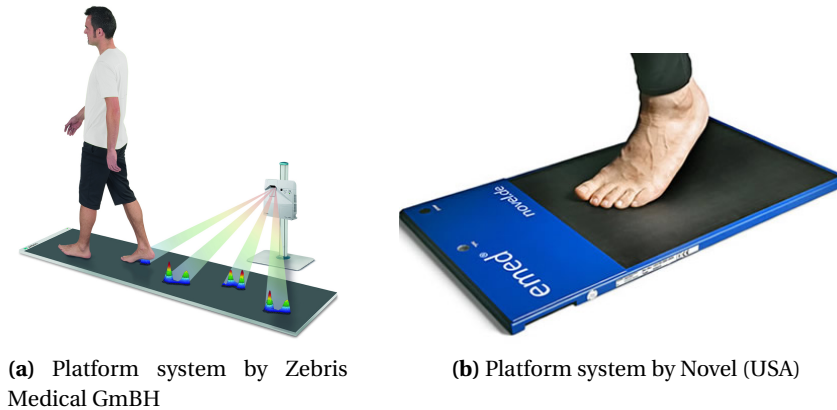


Figure 4.2: Examples of platform based pressure measurement systems.

In Shoe Systems

Due to limitations imposed by platform systems, more and more literature targeting in-shoe systems is being published. This section reviews few of such studies found in literature.

Tan et al. (2015) presented insole system made up from carbon embedded piezo-resistive material sandwiched between two layers of conducting electrodes. The horizontal electrode layer consists of 15 elements whereas vertical electrode layer consists 5 elements resulting in total 75 sensing nodes. The data is sampled at 13Hz sampling frequency and transmitted to PC wirelessly via Arduino+Bluetooth setup . Although this system has 75 sensing nodes, it is mentioned in the paper that system was capable of reading only one datum at a time causing significant data discrepancy in the readings due to time difference between first and last reading. Authors used time interpolation at all nodes to obtain more accurate depiction of data. The study also does not provide any picture of final complete setup for comparison.

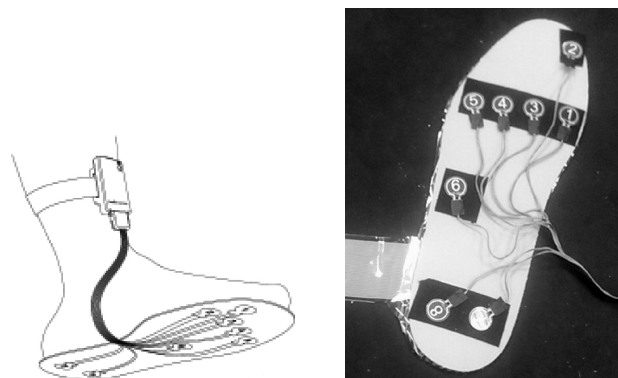


Figure 4.3: WalkinSense pressure measurement system. (Healy et al. (2012))

Healy et al. (2012) presented a research in which authors claimed their custom developed system is better than commercially available systems. The system shown in Figure 4.3 called ‘WalkinSense’ consists of eight pressure sensors and data acquisition system. Authors compared this system with commercial F-Scan system by Tekscan[®]. However, study has reported some inconsistencies in readings and advised further investigation with large sample size.

A fabric sensing array based insole design is presented in study by Shu et al. (2010). The fabric sensor technology presented is based on carbon black based silicon which is developed by author’s research group. This sensor can be used to measure pressures from 10 Pa upto 800kPa. Insole design consists six of such fabric sensing array sensors and wireless transmission circuit shown in Figure 4.4a. The sensor outputs are used without any signal conditioning providing 100 Hz sampling frequency with 2kPa resolution and $\pm 5\%$ accuracy. Interestingly authors also tried to calculate amount of weight supported by the sensor positions by taking average of pressure and area.



(a) Insole systems developed by Shu et al. (2010)



(b) SmartSox system based on Fiber Brag Grating (Najafi et al. (2017)).

Figure 4.4: Different pressure measurement systems in literature

Najafi et al. (2017) presented sock to measure temperature, pressure and toe angle for diabetic foot risk. Novelty in this sock design lies in the use of optical fiber sensors for all the measurements. The sock design uses very thin (<0.3 mm) fiber optical sensors based on Fiber Bragg Gratings (FBGs) at five locations. The measurement can be achieved by changing properties of fiber such that change in parameter to be monitor modulates intensity, phase, polarisation or transit time of the light. The system is shown in Figure 4.4b. Use of FBG based system provided many advantages such as electrical insulation, chemical resistance, elimination of frequent calibration and temperature independence. However long wires attached to the systems limit mobility and home or outdoor usage. Moreover experiments conducted in this study showed difference in temperature and pressure values between sock and reference system demanding more research in the sensor technology.

Perrier et al. (2014) proposed design of smart socks system using piezo-resistive and conductive fabric to measure pressure at eight different locations. Noteworthy thing about the paper is their focus on finding patient specific information. Since pressure measurements are dependent on the foot anatomy and hence they can vary from person to person. The work presented in the paper targets to extract patient specific internal foot strain and stress using finite element analysis method. They also designed a sock system including battery, MCU and Blue-

tooth module. However this study does not provide any information about characterization of the fabric sensors or the overall sock system.

Lin and Seet (2016) present battery free design of sock for plantar pressure measurements. This system can be solely powered by radio frequency (RF) energy harvested from RFID tag. The sock consists of four piezoelectric force sensor made out of fabric, however the response of the sensor is highly non-linear : resistance drops from 2.5k to 0.5k in just 300 kPa applied pressure and reaches to $\approx 0.2k$ at 1000 kPa. Furthermore due to limited battery capacity of RFID reader, only 40-80 readings can be obtained. But some of the noteworthy ideas such as energy harvesting, flexible PCB and removable interconnects are presented in this paper.

Hegde and Sazonov (2015) proposed design of wireless versatile insole monitoring system shown in Figure 4.5a in their study. Developed system comprises of three pressure sensors, accelerometer and gyroscope, ready-made Bluetooth module and battery. Their focus is on introducing new capabilities into the insole systems such as seamless wireless charging and over the air update capability.

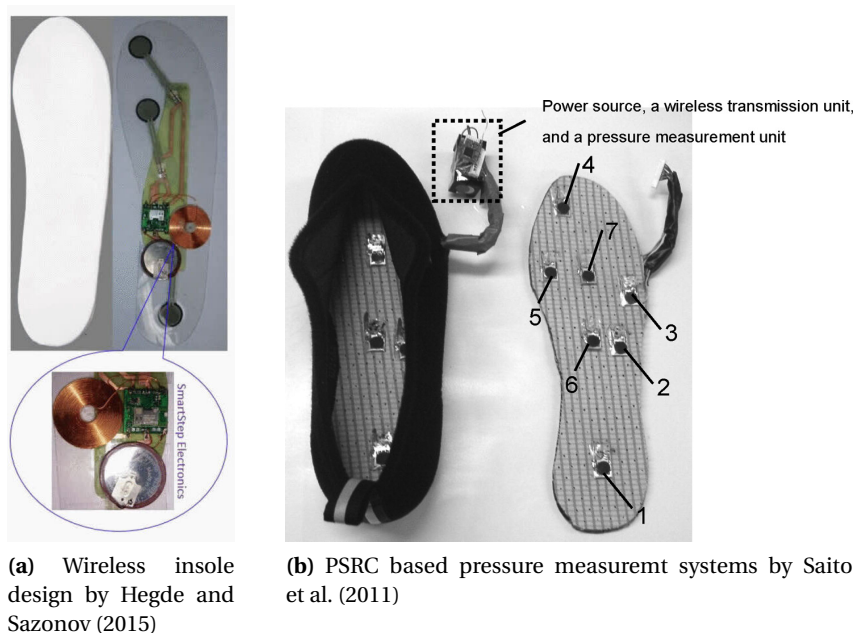


Figure 4.5: Different foot measurement systems found in literature.

Saito et al. (2011) used pressure sensitive conductive rubber (PSCR) sensors to measure the plantar pressure. Seven of these PSCRs were placed on the insole along with data acquisition system as shown in Figure 4.5b. This system weighs 160 grams, with costs around 1000 dollars and sampling frequency of 20 Hz.

Reyzelman et al. (2018) present observational study on effects of using temperature monitoring at home. The authors present the designed sock with neurofabric temperature sensors with $0.2^{\circ}C$ of accuracy of readings taken. The readings are taken at six different foot locations at time interval of 10 seconds. The sock is washable and connects to cellphone using Bluetooth. This is the only research found in literature that solely focuses on developing hardware targeted at temperature readings.

Finally, study by Coates et al. (2016) is the most exhaustive system found in the literature targeted towards multi-modal skin sensing for diabetic foot. Authors use accelerometer, humidity, force, temperature, galvanic skin response and bio-impedance to characterize skin condition. This system shown in Figure uses Arduino and Raspberry pi interface for data acquisition at 20Hz frequency.



Figure 4.6: Different foot measurement systems found in literature.

The recent trend of the research is shifting towards design of socks based systems from design of shoe based system. Although these sock or shoe systems have low spatial resolution as compared to commercial insole or platform systems, they offer several advantages as well. These systems are practical as sock can be used in conjunction with or without different footwear giving more freedom to the user. However most of the studies presented on sock design try to use custom fabric sensor which has in-adequate pressure range or very few sensor locations. Moreover, very few studies have been found that try to embed pressure, sensor and other sensors together in the sock. This research tries to fill this void by designing such sock system using commercially available sensor technology.

4.3 Market research for socks

Once decision on sock design is finalized, a short survey about commercially available socks for diabetic ulcer prediction is conducted to find out characteristics of such systems. Results of this survey are summarised below:

1. Taxisense used their patented fabric technology to develop a washable pressure sensing sock called 'Taxisocks'TM. However these socks are not for sale and can be only used in collaboration with the company.
2. Alpha-fit, a Germany based company has developed a 3D pressure sense mesh socks in 2012. However this sock is not available in market for sale yet.
3. Sensoria is US based fitness company. The smart sock system is aimed to provide information about running including step counting, speed, calories, altitude and distance tracking and overall score. This sock deploys three pressures sensors at the plantar side of the foot and costs \$200 for complete system.
4. Siren is the only commercially available socks targeted towards diabetic patients. Fully washable Siren socks monitors foot temperature changes to predict diabetic ulcer and available commercially as subscription based service. These socks can be only obtained as prescription from doctor and official pricing is not available on the website. The literature study by Reyzelman et al. (2018) is done using these socks.

4.3.1 Research Novelty

As per foot parameters identified in the previous chapter, it has been found that there are very few sock designs targeted towards diabetic foot monitoring parameters. Sock design is pre-

ferred to shoe or insole design as it can cover more use-case scenarios both indoor and outdoors.

Waaajman et al. (2014) have demonstrated the use of temperature for ulcer prediction but their sock does not monitor any other parameter. Najafi et al. (2017) have designed sock that monitors foot pressure and temperature using Fiber Bragg Grating however, the sock design is not comfortable and continuous monitoring is not possible.

Although there are few examples of commercial socks, only Siren and Alpha-Fit socks are capable of detecting abnormal changes in temperature or pressure respectively. These socks just target one parameter each. Moreover, none of these products give any information about number of sensors, spatial resolution, measurement range and accuracy of the system. Furthermore, out of these socks only Siren Socks are available in the US on doctor's prescription.

There is a lack of sock design targeting combination of diabetic foot predictors outlined in previous chapter. This shows that there is room for a novel sock design using temperature, pressure and possibly other parameters for DFU prediction.

4.4 Summary

- Commercially available systems for pressure measurements are expensive and do not provide any information apart from pressure.
- Recent research trend shows inclination towards sock-based wearable systems however, there is a research gap for use of multiple parameters in sock system.
- Few such socks are commercially available. These systems only target one parameter and does not provide any information about the measurement system.
- Hence, sock based wearable design incorporating multiple diabetic foot indicators has better prospects and offers several advantages of platform or shoe-based systems.

5 Hardware Design Exploration

In previous chapter we looked at state of the art solutions for diabetic ulcer prediction, and based on the observations and limitations, design decision of sock development is made. To develop smart-sock prototype it is essential to obtain requirements for hardware and software design. This chapter deals with overall design decisions in hardware design followed by calibration and conditioning of the selected sensors.

5.1 Requirements

Hardware design requirements are decided on the basis of scientific as well as practical aspects of the sock design. These requirements are summarised as below:

- Sensors should be able to measure in required range of values for temperature and pressure readings.
- Sensors data must be reproducible and repeatable.
- Errors in readings must be within limits.
- Resolution requirements must be met.
- Sensors must be flexible enough to be embedded in sock.
- Sensors should not cause any hindrance to the normal movement of the leg.
- Sensor should not inflict any kind of force or damage to the feet.
- Overall circuit must consume low power for long operation hours on battery.
- Size of the circuit must be as small as possible.

5.2 Choice of Sensors

In addition to the requirements mentioned in previous section, there are also specific requirements depending on the parameter to be measured. There are different type of sensor technologies available that can be used to measure a single parameter. Hence it is important to analyse these sensor technologies and select the best suitable sensors for required application. This section provides information about the requirements, sensing technologies and best suitable technology for temperature and pressure sensors.

5.2.1 Pressure Sensor Selection

Requirements:

- Range: 0-1000 kPa (Razak et al., 2012).
- Sensing area: large area underestimates peak pressure where as too small area leads to inaccurate estimate of peak pressure. Sensor area should be minimum 5*5 mm to be a stand-alone sensor (Razak et al., 2012).
- Linear response leading to simple Conditioning circuit.
- Sensors must be flexible enough to be embedded in sock.
- Suitable for low power operation

Before diving into sensor selection, a short survey of different force/pressure sensing technologies is performed. These technologies are listed below:

Capacitive Force Sensors

Capacitance is function of surface area of the capacitor, thickness of dielectric and properties of dielectric. A capacitive force sensor can be made by making one of these properties a function of applied force. Typically, capacitive force sensors change the thickness of dielectric. Two conductive planes are separated by dielectric to form a capacitor. When force is applied distance between two plates is reduced thereby increasing capacitance. This change in capacitance can then be translated to applied force using conditioning circuits. Gonçalves et al. (2018) provide comparison of different textile capacitive sensors production techniques.

Optical Force Sensors

Optical sensor measure change in light intensity passing through the fiber as result of the exerted force (Gonçalves et al., 2018). Such systems use Fiber Bragg Grating (FBG) technique shown in Figure 5.1. These systems consist of Light emitting diode (LED) on one end which transmits light through the thin fiber, and a photo-diode to detect the light on the other end. Movement, displacement or force changes the amplitude of received signal at the photo-diode. Optical sensors have an advantage to be electrically non conductive (isolated). Such fiber systems can be built in diameters in range of microns reducing size of the sensor. However they are fragile and require complex conditioning circuits.

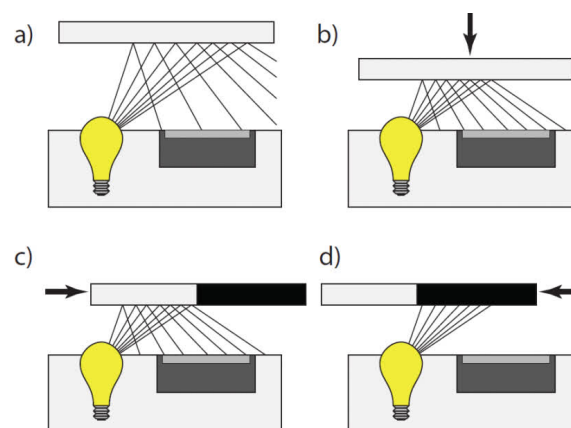


Figure 5.1: An Example of working principle of optical force sensor. Any movement due to load (a-b) or shear force (c-d) affects the intensity of received light at the detector. (adopted from (Lincoln et al., 2012))

Force Sensitive Sensors

Force Sensitive Resistors (FSR) are in essence piezo-resistive devices whose resistance linearly decreases as the force applied on them increases. FSRs shown in Figure 5.2 consists of semi-conductive ink layer contained between two thin substrates. The piezo resistive layer lies in between two conductive areas. When unloaded this layer exhibits very high resistance in orders of Mega-ohm ($M\Omega$). As the force gets applied, resistance of the layer changes and resultant voltage or current changes can be observed between two conductor leads. Since conductive and piezo-resistive layers can be made very thin, FSRs are thin and flexible. Furthermore, they are simple passive elements with linear response and require very simple conditioning circuit. There are different FSR modules available in different shapes, sensing areas and sensing capabilities. These characteristics make them suitable in many medical applications.

Considering all sensing technologies, a search was performed to find commercially available sensors. FSRs are selected for further process as they offer :

- Thin and flexible design (0.2mm thickness).

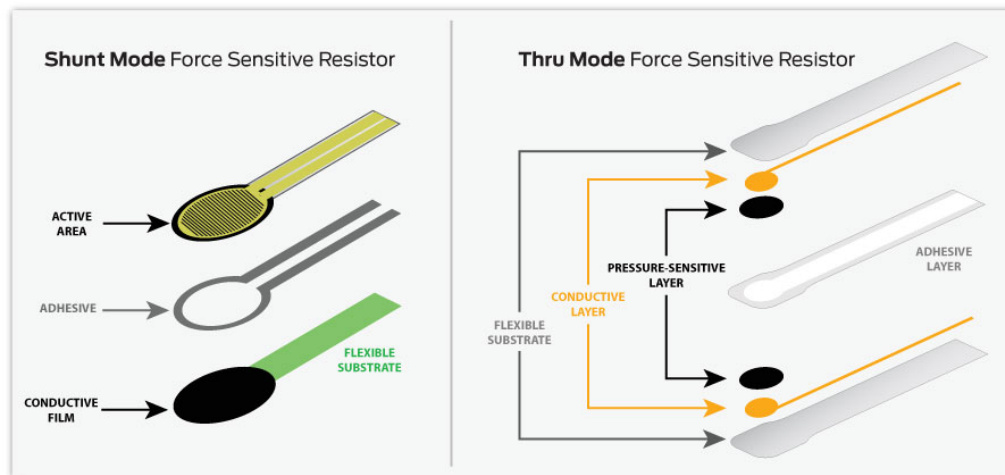


Figure 5.2: Basic construction of Shunt and Thru mode force sensing resistors. The resistance of pressure sensitive layer changes according to applied pressure. (Taken from Tekscan (2019))

- ability to measure required range of pressure values (upto 4448N).
- Easy to integrate.
- Linear output with simple conditioning circuit.
- Suitable for low power design.
- Such sensors are widely used and characterised in different studies in literature marking their suitability for foot pressure measurement.

5.2.2 Temperature Sensor Selection

Requirements

- Accuracy: $\pm 0.5^{\circ}\text{C}$
- Temperature Range: $25 - 45^{\circ}\text{C}$
- Flexible
- Suitable for low power operation.

Thermocouples

A thermocouple is an electrical device which is constructed by joining two dissimilar conducting metals. When two dissimilar metals at different temperatures are connected together, they form an electrical junction. A small voltage is generated across this electrical junction which is a function of the temperature. This is called Seebeck effect. Thermocouples utilize the Seebeck effect by using one reference junction (cold junction) and one measuring junction (hot junction) and then observing the generated thermo-electric voltage to calculate temperature at measuring junction. This process is illustrated in Figure 5.3. There are many different types of thermocouples available based on combination of conductors used. These different combinations provide different temperature measurement ranges. The "K" type thermocouple is most widely used. It is made up of Nickel Chromium / Nickel Aluminium and can measure temperatures from -180°C to 1300°C . Since, generated thermo-electric voltage is very small, a precise low noise amplification stage is required. However, they have disadvantages such as reduced accuracy, noise susceptibility, and undesired junction formation between PCB and thermocouple.

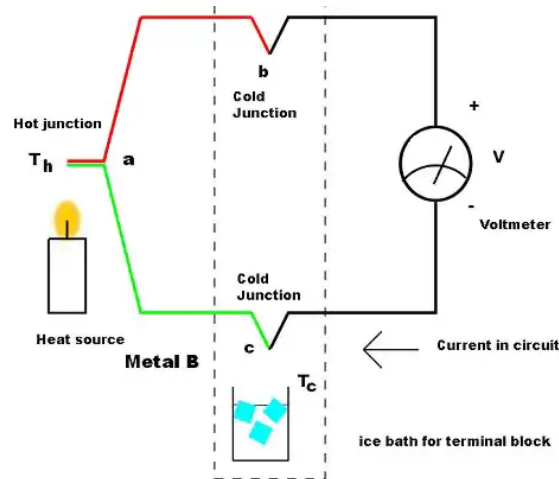


Figure 5.3: Working principle of thermocouple. (adopted from (Jon Gabay, 2013))

Resistor Temperature Detector

As temperature changes, resistance of material changes. Resistor Temperature Detectors (RTDs) utilize this phenomenon to measure temperature changes. The RTDs are usually made up of platinum, copper and nickel. They exhibit high degree of linearity which means change in resistance is directly proportional to change in temperature. If a known current is passed through the RTDs, measured voltage can provide current value of resistance which in turn can be used to calculate temperature. There are two, three and four wire configuration available where four wire configuration provides best accuracy of all. RTDs are highly precise and repeatable however they respond to changes slowly.

Semiconductor ICs

Semiconductor based temperature sensor ICs come in two different types: local temperature sensor and remote digital temperature sensor. Local temperature sensors are ICs that measure their own die temperature by using the physical properties of a transistor. Local temperature sensors can be obtained in analog or digital output. These sensors are used to sense the temperature on printed circuit boards or the ambient air around it (Jason Gums, 2018). Remote digital temperature sensors measure the temperature of an external transistor. Working principle of remote digital temperature sensor is similar to local temperature sensors. Only difference is that the actual position of sensor is away from the chip rather than inside the chip. Nowadays, many microprocessors and FPGAs also come with bipolar sensing transistor to measure die temperature of the IC (Jason Gums, 2018).

Thermistors

Thermistors work on same principle as RTDs but the construction is different. Each thermistor has temperature co-efficient associated with it indicating degree of change in resistance with change in temperature. There are two types of thermistors: Positive Temperature Coefficient (PTC) Thermistors and Negative Temperature Coefficient (NTC) Thermistors. Resistance of PTC thermistors increases as temperature increases and NTC exhibit opposite behaviour. NTC thermistors are most common and made from oxides of cobalt, nickel, iron or manganese.

Thermistors have quick response, are reliable, robust and cost less thus making them popular for general use. Figure 5.4 shows typical resistance versus temperature variation of thermistor. Although this change in resistor is non-linear, it can be made linear by using simple signal conditioning circuit.

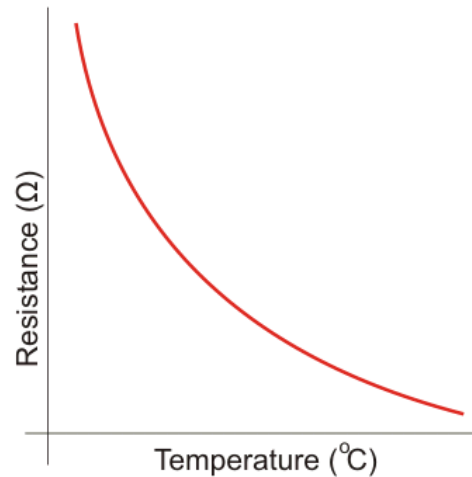


Figure 5.4: Example of non-linear Resistance Vs Temperature characteristics of NTC thermistor.

5.3 Accelerometer Selection

Pressure alone can not be used to detect or predict abnormal foot condition. The abnormal distribution of the pressure can be because of certain posture or physical activity. Hence some additional information is required to accurately analyse pressure readings obtained from the sensors. Accelerometer is used for precisely this purpose.

There are many studies found in literature that solely use accelerometer for gait patterns. Such studies require precise accelerometer with high precision. However since accelerometer will be used as supporting data for pressure readings, restrictions are not very strict.

Keeping this in mind a short survey of accelerometers is conducted. Accelerometer module based on MMA8451 is selected as it provides following features:

- 14 bit resolution.
- Output data rates (ODR) from 1.56 Hz to 800 Hz.
- $\pm 2g / \pm 4g / \pm 8g$ selectable dynamic range.
- Low power operation (1.95-3.6 V supply voltage)
- I²C digital output interface.

5.4 Heart-Rate Monitoring

Foot Perfusion test is performed as part of clinical tests for diabetic patients. This test is performed to evaluate the effective blood circulation of the foot. To monitor blood perfusion, decision to add Heart-Rate Monitor is taken. Heart rate monitors can provide information about pulse and oxygen saturation (SpO₂) of the blood which can help in extracting foot perfusion information.

Optical heart rate sensor which are most commonly used in embedded solutions, work on based on photoplethysmography (PPG) process. This method works by shining light into the skin and then measuring the light scattered due to blood flow. When the blood flow changes due to physiological changes such as blood pulse rate or change in blood volume, light shown on the skin also changes in predictable manner. This information can be used to extract information about blood flow of the body such as pulse rate or oxygen saturation.

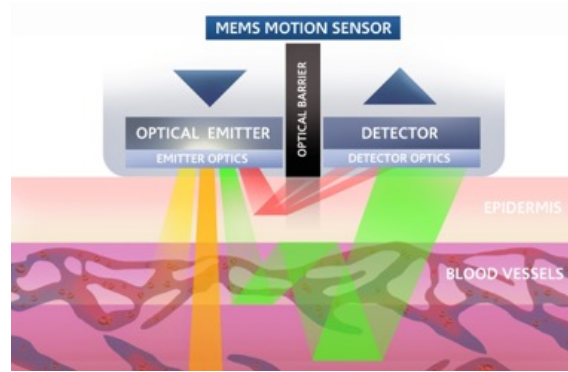


Figure 5.5: Working principal of heart-rate sensor

For the testing of heart rate monitor feasibility, MAX30102, a low power heart-rate and SpO₂ monitor was selected. Manufacturer of the sensor (Maxim Integrated) also provided sample implementation of heart-rate algorithm to facilitate sensor integration and adoption.

There are two areas of the foot where pulse can be detected. Heart-Rate sensor is placed at both sites to test the feasibility of the sensor integration. However it is found that sensor provided inconsistent results. On further analysis two possible causes are discovered:

- Heart-Rate sensor is very sensitive to any movement of the sensor from the skin surface. As it can be seen in Figure 5.5, if there is disturbance, it directly affect scattered and received signal at the detector. This results in erroneous readings.
- Foot structure is filled with tendons and ligaments. Due to this it is difficult to locate the arteries which intern affects the positioning of sensor .
- There are algorithms available which can use accelerometer readings to compensate for the movement of the sensor. However these algorithms are mostly used in commercial systems and not available in open implementation.

These encountered issues make inclusion of heart-rate sensor infeasible. Hence it is not considered for integration in the sock design.

5.5 Sensor Conditioning and Calibration

Once sensor technology is selected and sensors are finalized it is important to characterize these sensors before integrating into the system. This section provides information about calibration of sensor and reasons for using conditioning circuit.

5.5.1 Pressure

As mentioned in previous section, force sensing resistor is used to measure the exerted force. The Interlink FSR is first characterised using simple resistor divider circuit. As it will become apparent, both the sensor and circuit are not able to meet the design requirement. The new sensor along with the conditioning circuit is then characterized to plot calibration curve.

Simple Circuit

To analyse FSR (Interlink 402), a test is conducted with very simple resistor divider network. FSR is connected to ground on one end and its other end is connected to 10k Ω resistor which is then connected to 3.3V supply. Analog reading is taken from the junction between FSR and 10k Ω . As force exerted on FSR increases, its resistance decreases showing higher output voltage readings. Block diagram of test setup is shown in Figure 5.6. To mimic exerting force of known values, weight of known values is kept on the sensor using 3D printed test jig. ADC readings

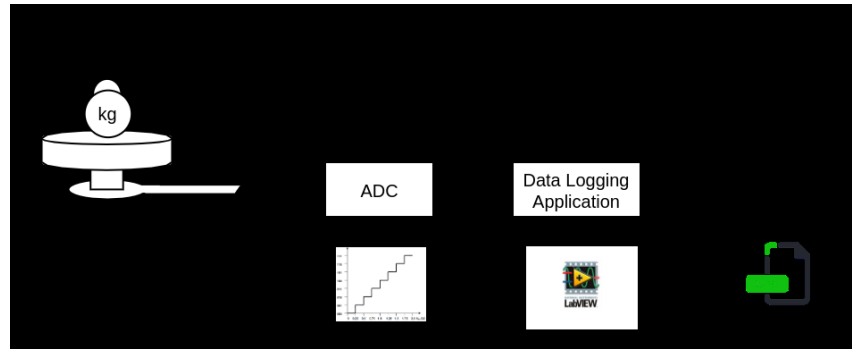


Figure 5.6: Block diagram of pressure sensor calibration setup.

were transmitted to PC over UART where a simple data acquisition program was developed using LabView to log the data.

Weight (grams)	Readings	Avg ADC Readings (Raw)	Avg ADC Readings (V)	Pressure (kPa)
1000	17	2736.7647	2.8990	19.35
2300	27	2751.0740	2.9149	44.50
3000	29	2952.7241	3.1289	58.05
4000	34	2980.7670	3.1583	77.40
5000	29	2996.7037	3.1750	96.75
6250	40	3019.5750	3.1991	120.93
7300	31	3022.4193	3.2020	141.25
8000	35	3024.0857	3.2038	154.80
9250	24	3024.6667	3.2044	178.99
12250	8	3033.2500	3.2134	237.04

Table 5.1: FSR Readings for resistor divider network setup

Results of ADC readings for different weights are summarised in Table 5.1. For each weight multiple readings are obtained and average of these readings is used to calculate pressure. Pressure is calculated by first calculating force ($\text{Weight} * 9.8$ (gravity)) and this calculated force is then divided by area of the sensor to obtain pressure. Plot of ADC reading vs Pressure characteristics is depicted in Figure 5.7. It can be easily observed that the response of FSR is non-linear and output saturates as we reach higher weights.

This behaviour can be traced back to following factors:

- Inadequate test-jig design which does not exert weight effectively and equally on sensor surface.
- Simple circuit without any sensor conditioning.
- Limited force range of sensor.

Both of these limitations were addressed in new tests performed as explained in following section.

Sensor Readings With Conditioning Circuit

Simple voltage divider network used for previous testing does not provide linear output. Furthermore, range of FSR (Interlink 402) was not sufficient to sense required pressure range. To

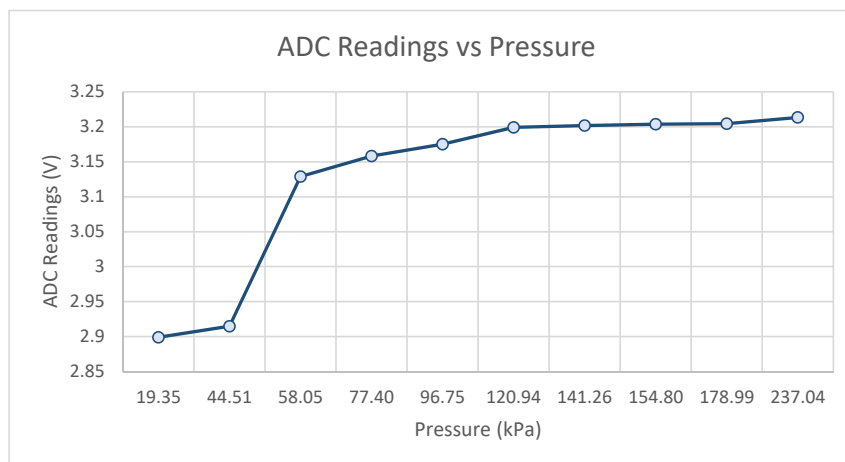


Figure 5.7: Plot of ADC Readings obtained for different pressure values exerted on the FSR.

overcome these limitations, new FSR sensor Flexiforce A301 from Tekscan is used. This sensor can measure up-to 4448N force with sensing area of 9.5mm diameter. Furthermore, signal conditioning circuit as shown in Figure 5.8 is also designed to drive FSR.

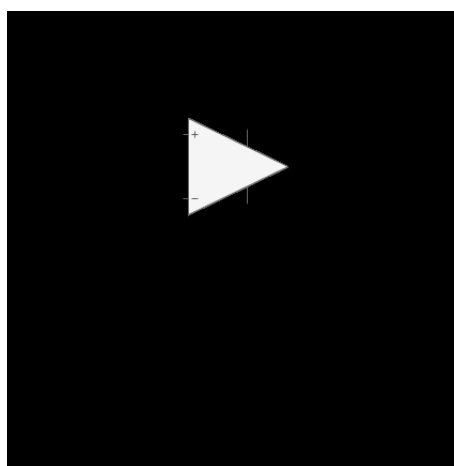


Figure 5.8: FSR conditioning circuit for low/battery powered devices.

The op-amp circuit shown in Figure is a simple inverting op-amp configuration with reference voltage provided at non-inverting terminal. Due to virtual ground, both terminals of the op amp will try to be at the same voltage. This means op-amp will try to make voltage at inverting terminal equal to V_{ref} . Since op-amp does not draw any input current, the voltage at inverting terminal is essentially voltage across FSR. This allows to see feedback circuit as voltage divider network.

This results in voltage at inverting input (and across FSR essentially) as:

$$V_{FSR} = V_{out} * \frac{R_{FSR}}{R_{FSR} + R_{feedback}} \quad (5.1)$$

with simple manipulation following relation between input and output can be obtained:

$$V_{out} = V_{ref} * \left(1 + \frac{R_{feedback}}{R_{FSR}}\right) \quad (5.2)$$

Equation 5.2 shows that output voltage is dependent upon two variables: R_{FSR} and $R_{feedback}$. According to sensor manufacturer's (Tekscan) user guide, this value should be adjusted using

100k potentiometer. The value of this feedback resistor is used to decide sensitivity and range of the FSR. It is found that R_{feedback} resistor of $100k\Omega$ provides better sensitivity within range of interest.

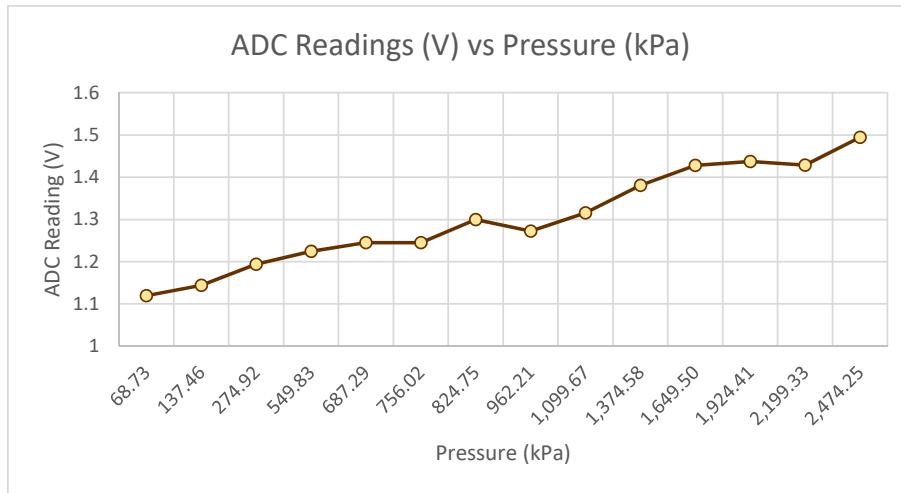


Figure 5.9: Calibration curve for FSR ADC Readings versus weight with $R_{\text{feedback}} = 50k\Omega$

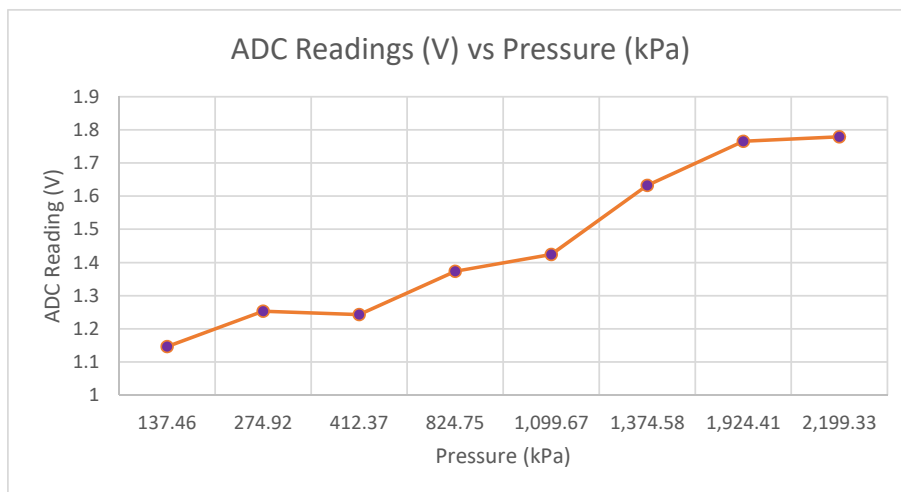


Figure 5.10: Calibration curve for FSR ADC Readings versus weight with $R_{\text{feedback}} = 100k\Omega$

Once value of R_{feedback} is fixed, input-output voltage is entirely function of R_{FSR} defined by equation 5.2. In addition to this, use of op-amp also provides following advantages:

- High input impedance
- Low output impedance reducing loading effect.
- Better Signal to noise ratio

The problems in the simple sensor circuit (without signal conditioning) are addressed as follows:

- A new FSR sensor with greater force sensing range is selected.
- Inverting op-amp configuration with reference voltage at non-inverting terminal is selected as conditioning circuit according to guidelines provided in data-sheet (Figure 5.8).

- Improved 3D printed test bed is designed to ensure uniform force distribution on the sensor as well as to make sure sensor is held at fixed place during the experiment.

The new sensor and conditioning circuit is then subjected to similar tests to acquire readings for different weights. As with the previous experiment, multiple ADC readings were logged and average value is used for plotting the graph.

Two sets of readings were obtained for feedback resistor values of $50k\Omega$ and $100k\Omega$. The logged data for $R_{\text{feedback}} = 50k\Omega$ is summarised in Table 5.2. Plot of ADC readings for different weights is illustrated in Figure 5.9 ($R_{\text{feedback}} = 50k\Omega$) and Figure 5.10 ($R_{\text{feedback}} = 100k\Omega$).

Analysing both graphs provides following information:

- New FSR and conditioning circuit provide better force sensing range ($>18\text{kg}$ ($\approx 1400\text{kPa}$))
- FSR follows near linear response.
- Feedback resistor value of $100k\Omega$ provides better output range resolution (1083-1680) than $50k\Omega$ resistor (1081-1349) for same pressure range.

Weight (grams)	Readings	Avg ADC Readings (Raw)	Avg ADC Readings (V)	Pressure (kPa)
500	30	1058.267	1.1196	68.72909
1000	32	1081.688	1.1442	137.4582
2000	105	1128.229	1.1941	274.9164
4000	44	1157.432	1.2248	549.8328
5000	40	1177.025	1.2454	687.2909
5500	35	1181.342	1.245	756.02
6000	49	1227.673	1.3	824.7491
7000	33	1201.667	1.2723	962.2073
8000	60	1243.083	1.3158	1099.666
10000	47	1304.042	1.3809	1374.582
12000	32	1348.25	1.4279	1649.498
14000	52	1357.788	1.4373	1924.415
16000	24	1349.667	1.4288	2199.331
18000	37	1411.027	1.4942	2474.247

Table 5.2: FSR Readings with $R_{\text{feedback}} = 50k\Omega$

Weight (grams)	Readings	Avg ADC Readings (Raw)	Avg ADC Readings (V)	Pressure (kPa)
1000	15	1083.467	1.1461	137.4582
2000	35	1184.657	1.2534	274.9164
3000	32	1202.688	1.2434	412.3746
6000	25	1296.96	1.3733	824.7491
8000	51	1345.431	1.4243	1099.666
10000	20	1541.65	1.6324	1374.582
14000	26	1666.423	1.7655	1924.415
16000	37	1680.114	1.7789	2199.331

Table 5.3: FSR Readings with $R_{\text{feedback}} = 100k\Omega$

5.5.2 Temperature

In this section, characterization of temperature sensor (Semitech 103JT) is explained. To improve the performance, conditioning circuit is used and new setup is also evaluated to obtained calibration curve.

Simple Circuit

Temperature sensing is done using 103JT-050 Thermister from Semitec. 103JT has thickness of 500 microns, dynamic range of -50 to +125 °C and room temperature resistance (R_{25}) of $10k\Omega \pm 1\%$. Since range of interest is between 25-45 degrees, test was designed to focus on obtaining temperature readings in this range.

Temperature calculations are done using Steinhart Equation (equation 5.3) which is widely accepted across industry and considered as best empirical mathematical expression for approximating non linear behaviour (Bonnie C. Baker, 2004).

$$T = \frac{1}{A + B * \ln(R) + C * (\ln(R))^3} \quad (5.3)$$

Parameters A,B and C can be calculated using three known resistor values for three different temperatures spaced at least 10 degrees apart. Since our range of interest of temperature is within 30-50 degrees, we will calculate these parameters for this range by taking given resistor readings at 30,40 and 50 degrees in the datasheet (Appendix B).

$$\frac{1}{T} = A + B * \ln(R) + C * (\ln(R))^3 \quad (5.4)$$

For $T = 30^\circ$ (303.25 Kelvin):

$$\begin{aligned} \frac{1}{T_{30}} &= A + B * \ln(R_{30}) + C * (\ln(R_{30}))^3 \\ \frac{1}{303.25} &= A + B * \ln(8301) + C * (\ln(8301))^3 \\ 3.2976E - 3 &= A + B * 9.0241 + C * 734.8796 \end{aligned} \quad (5.5)$$

For $T = 40^\circ$ (313.25 Kelvin):

$$\begin{aligned} \frac{1}{T_{40}} &= A + B * \ln(R_{40}) + C * (\ln(R_{40}))^3 \\ \frac{1}{313.25} &= A + B * \ln(5811) + C * (\ln(5811))^3 \\ 3.1923E - 3 &= A + B * 8.6675 + C * 651.1525 \end{aligned} \quad (5.6)$$

For $T = 50^\circ$ (323.25 Kelvin):

$$\begin{aligned} \frac{1}{T_{50}} &= A + B * \ln(R_{50}) + C * (\ln(R_{50}))^3 \\ \frac{1}{323.25} &= A + B * \ln(4147) + C * (\ln(4147))^3 \\ 3.0935E - 3 &= A + B * 8.3301 + C * 578.0388 \end{aligned} \quad (5.7)$$

Solving three equations obtained (equation 5.5,5.6 & 5.7), we can get values for three unknowns (A,B,C). The solved values are as follows:

$$\begin{aligned} A &= 0.8211E - 3 \\ B &= 0.2633E - 3 \\ C &= 1.3602E - 7 \end{aligned} \quad (5.8)$$

Now we can calculate temperature (in kelvin) for any thermistor reading using equation 5.3 and values of A,B,C obtained in equation (5.8) as follows:

$$T = \frac{1}{A + B * \ln(R) + C * (\ln(R))^3}$$

$$T = \frac{1}{0.8211E-3 + 0.2633E-3 * \ln(R) + 1.3602E-7 * (\ln(R))^3}$$

$$T = \frac{1000}{0.8211 + 0.2633 * \ln(R) + 1.3602E-4 * (\ln(R))^3} \quad (5.9)$$

Test Setup and procedure

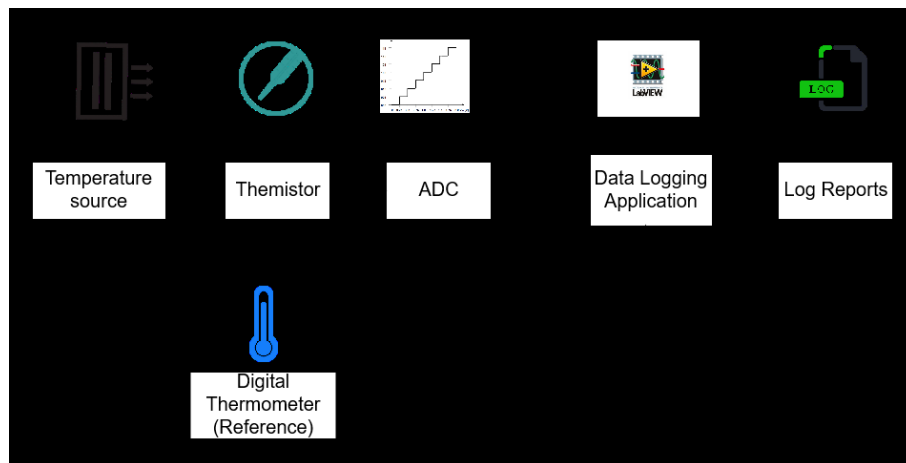


Figure 5.11: Block diagram of temperature sensor calibration setup



Figure 5.12: Test setup for temperature sensor calibration.

The basic setup used to perform these test is shown in Figure 5.12 and Figure 5.12. Test setup-involves a hot plate with temperature control, a glass beaker with clean water and a digital thermometer for reference temperature. For each reading water temperature is monitored to be stable for at least 5 seconds. Once temperature is stable, ADC readings are recorded with 1Hz frequency. $\pm 0.1^\circ\text{C}$ variation in water temperature is allowed while taking the readings. At least 10 samples are collected per temperature setting.

After all the readings are recorded, script is written in Scilab to take average of all the readings for particular temperature, calculate sensor resistance from it and then calculate sensed temperature using equation 5.9. The results of this process are shown in Table 5.4.

T_{Ref}	Total Readings	Raw ADC Reading (μV)	ADC (V)	R_{sensor}	$T_{calculated}$	Error($^{\circ}C$)	Error (%)
32.2	14	1829430	1.829430	8083.40	30.85	1.34	4.1925
34.6	14	1904884	1.904884	7323.88	33.45	1.14	3.3237
36.4	17	1916691	1.916691	7217.17	33.86	2.53	6.9780
37.8	13	1982516	1.982516	6645.50	36.19	1.6	4.2592
38.3	23	1994430	1.994430	6546.07	36.62	1.67	4.3864
40	25	2062319	2.062319	6001.40	39.10	0.89	2.25
40.5	30	2073520	2.073520	5914.96	39.52	0.98	2.4197
41	23	2078390	2.072390	5877.67	39.70	1.29	3.1707
42.1	30	2099631	2.099361	5717.04	40.50	1.56	3.800
43.1	38	2139195	2.149195	5426.36	42.01	1.08	2.5290
44.1	25	2160940	2.160940	5271.13	42.86	1.24	2.8117
45	20	2186069	2.186069	5095.58	43.85	1.15	2.5555

Table 5.4: Temperature sensor calibration without conditioning circuit.

Error	$^{\circ}C$	%
Max	2.54	6.978
Min	0.9	2.25
Avg	1.3825	3.5564
Std. Deviation	0.4415	1.322

Table 5.5: Statistics of calibration test without conditioning circuit.

Analysis of test

- It can be clearly observed from the Table 5.4 and Table 5.5 that average temperature difference of $1.38^{\circ}C$ exist between thermometer and the sensor.
- Maximum Error is $2.54^{\circ}C$.
- Since we want to measure temperature difference $> 2^{\circ}C$, maximum error in temperature difference will be 5.08 and average error will be 2.76 making this circuit unusable for proposed design.
- Thermometer readings consistently show higher temperature than the sensor. This can be contributed to following reasons.
 - In Figure 5.12, it can be seen that tip of thermometer is well below the tip of the sensor.
 - Temperature gradient exists in the water while heating the water. This can be avoided by stirring the water.
 - Experiment uses hot plate for heating water which is not very accurate and affected by surrounding environment as opposed to controlled environment test.

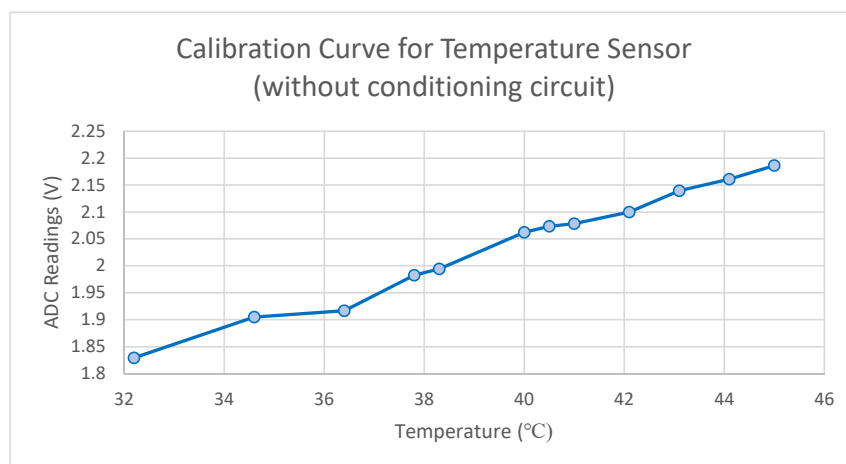


Figure 5.13: Temperature calibration curve for temperature sensor without conditioning circuit.

With Conditioning

Since FSR and thermistors are essentially both variable resistors (with resistance dependent on different physical parameters), conditioning circuit used for FSR conditioning can be also used for NTC thermistor with some modifications. Considering this, conditioning circuit similar to shown in Figure 5.8 and equation 5.2 can be used. Only thing that needs to be adjusted is value of R_{feedback} .

Sensor resistance of NTC thermistor in range of interest are in few kilo-ohms as compared to Mega-ohm resistance of FSR thermistor. Hence, conditioning circuit of NTC thermistor needs smaller R_{feedback} than FSR conditioning circuit. This value is set to $20k\Omega$ as it provides better resolution in required temperature range (this is obtained from experimentation with R_{feedback} values).

The test is performed with this new conditioning circuit and similar test environment as previous test. This time thermometer tip and sensor were kept at similar height to mitigate errors due to temperature gradient in water. Table 5.6 shows selected readings obtained while conducting the experiment. Full set of readings can be found in Appendix A. Temperature verses voltage readings plot is shown in Figure 5.14.

T_{Ref}	Sample Count	Raw ADC Reading	ADC (V)	R_{sensor}	$T_{\text{calculated}}$	Error (°C)	Error (%)
25.1	22	1877.0909	1.98681	9903.4526	25.2960	-0.1960	0.7809
27.4	26	1988.8846	2.105252	9091.8400	27.5808	-0.1808	0.66
29.4	20	2101.65	2.224711	8397.7168	29.7300	-0.3300	1.1226
32.5	30	2262.0333	2.395224	7572.5093	32.5691	-0.0691	0.2128
35.1	16	2423.8125	2.566154	6893.4619	35.1880	-0.0880	0.2508
38.2	27	2623.4762	2.777913	6204.2209	38.1710	0.0290	0.075
40.2	24	2768.0417	2.931812	5783.9293	40.1852	0.0148	0.0368
41.1	31	2849.2258	3.01774	5573.1336	41.2604	-0.1604	0.3903
42.3	19	2945.9474	3.120008	5341.4460	42.4980	-0.1980	0.4682
44.5	14	3091.7143	3.274841	5025.1621	44.2921	0.2078	0.4671

Table 5.6: Selected test results for temperature sensor calibration using conditioning circuit. (For complete Table refer Appendix A).

From the Table 5.6, Table 5.7 and Figure 5.4, it can be observed that:

Error	°C	%
Max	0.207884624	1.122553086
Min	-0.33003061	0.036807396
Avg	-0.13474282	0.453319748
Std. Deviation	0.11085033	0.270649779

Table 5.7: Statistics of calibration test results using conditioning circuit.

- Sensor exhibits maximum error of only 1.12 % or just 0.2°C with average error of 0.13°C.
- Standard deviation of temperature readings is 0.11 showing high degree of stability of readings.
- Overall accuracy of sensor is well within required range of $\pm 0.5^\circ\text{C}$ for temperature range 25°C to 45°C.
- Plot of voltage vs temperature shows near linear characteristics further illustrating positive effect of conditioning circuit.
- Lastly it is important to note that, there might be still errors due to relatively simple test setup as well as errors in reference temperature readings (resolution : 0.1°C) .

results of simple temperature sensing circuit and conditioning circuit it is evident that conditioning circuit provides highly linear response. Moreover, average error in conditioning circuit is 0.13°C which means average error in temperature difference between two legs will be 0.26°C. This error is well below the 2°C temperature difference requirement and hence this circuit can be used for skin temperature measurement.

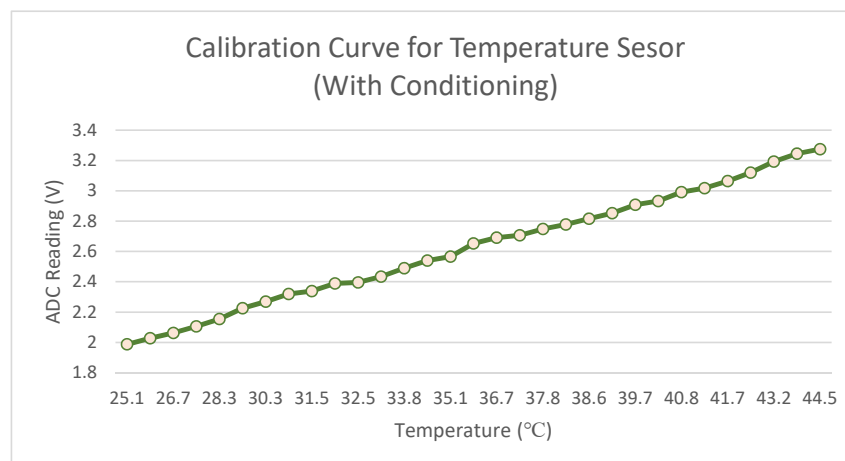


Figure 5.14: Temperature calibration curve for temperature sensor with conditioning circuit.

5.6 Communication Protocol Selection

Transfer of logged data to the receiving end can be performed using wired as well as wireless protocols. Wired protocols such as UART provide simple and reliable data transfer. However these require physical connection between two ends which limits range of movement and can greatly affect normal way of walking with risk of tripping over due to the connections.

Wireless protocols not only overcome these restrictions, but also provide better way to connect to different type of end devices as Bluetooth and WiFi capabilities become more commonplace.

Keeping this in mind, different wireless technologies suitable for data transfer are explored and summarised below.

Zigbee

Zigbee is a wireless technology built for integrating sensor network applications into the Internet of Things. This technology is highly inter-operable and is used to monitor and control sensor network applications. Zigbee is built on the universal IEEE 802.15.4 standard. It was developed to address the requirement of a cost-effective and standards-based wireless networking solution which also supports low power consumption, low data-rates, and is highly secure and reliable. Zigbee supports the self-healing mesh technology wherein a decentralized network for nodes is available, which enables them to find alternate routes in case of failure of one route. This also makes Zigbee a robust wireless technology.

ANT

Acronym ANT stands for "Advanced and Adaptive Network Technology". ANT target collection and transfer of sensor data with high degree of inter-operability. Nodes in the ANT network can act as transmitters, receivers, or transceivers to route traffic to other nodes. They can also decide when to transmit based on the activity of neighbouring nodes. ANT+ is second generation of ANT: a ultra low power version targeting health and fitness devices. ANT+ is designed for low bit-rate and low power sensor networks and works within short distances, typically less than 5 feet. Since all ANT+ devices are inter-operable, gadgets from different devices operate seamlessly with each other giving users freedom to design their own monitoring system.

Bluetooth

Bluetooth Low Energy (Bluetooth LE or BLE) is a wireless technology which caters to the needs of a wide range of applications. BLE is aimed at providing a communication range similar to previous versions of Bluetooth technologies but at reduced cost and power consumption. Currently in the industry, BLE SoCs supervised by Arm® Cortex®-M0, M3, M4, and M4F embedded processors are almost exclusively based on 2.4 GHz radios. These embedded processors are equipped with flash and RAM to aid stack firmware and application software storage and operation. Manufacturers also provide Software Development Kits (SDKs) and reference designs which makes it easier to work with BLE enabled SoCs.

WiFi

Wireless Fidelity (WiFi) is another standard-based wireless technology designed for large data transfer using high speed throughput. It is based on IEEE 802.11. Wifi is not suitable for low power operation. However, steps have been taken to improve the power consumption with amendments such as IEEE Standard 802.11v and IEEE 802.11ah (Wi-Fi "HaLow"). Wi-Fi "HaLow" was published in 2017 and operates in the 90 MHz ISM band. This leads to lower energy consumption and extended range compared to versions of Wi-Fi operating in the 2.4 and 5 GHz bands.

NFC

Near Field Communication (NFC) is the wireless sensor technology designed for short range communication. It operates in the 13.56 MHz ISM band where the transmit and receive loop antennas act as the primary and secondary windings of a transformer. At short distances, the magnetic field is stronger in comparison to the electric field and hence the former is used for data transfer. NFC provides data-rates upto 424 Kbits/sec with a maximum range of 10 cm. This makes NFC fall short in comparison to other wireless technologies presented previously. At the same time, NFC provides with the advantage of using "passive" devices (payment cards), which only become active in the presence of a closely located NFC powered device. NFC is

widely deployed in contact-less payment services and as a pairing method for other wireless technologies (such as BLE devices) since it is secure against man-in-the-middle attacks.

Comparison of Different Technologies

Parameter	Bluetooth	WiFi	Zigbee	ANT	NFC
Range	100	150	100	30	10 cm
Throughput	1 Mbits/sec	11 Mbits/sec	250 kbits/sec	20 kbits/s	424kbits/sec
Latency	2.5ms	1.5 ms	20ms	Nil*	NA
Power	30mA	-	30mA	-	50mA
Security	AES-128	AES	AES-128	AES	none

Table 5.8: Comparison of different wireless technologies. (Adopted from (Al-Sarawi et al., 2017; Patrick Mannion, 2017))

Selected Technology

After careful consideration of different technologies and the comparison provided in Table 5.8, Bluetooth LE is chosen as preferred communication protocol. The reasons for opting Bluetooth over other technologies are as follows:

- Good balance of throughput and power and range
- Low power
- Low latency
- Easy to integrate and interface with different end devices
- SDK, documentation and community support

5.7 MCU selection

After selection of Bluetooth as a preferred communication protocol, two options were available to integrate Bluetooth into the smart sock design: using Bluetooth enabled MCU or using separate Bluetooth module along with MCU. Bluetooth enabled MCUs are selected, as in general, they offer compact design with less additional components and better native library and tool support. Some of the requirements and comparison criteria for MCU selection are listed below:

Requirements

- On chip Bluetooth LE support.
- Compact Design with less additional components
- Support for SPI,I2C or other protocols for sensor integration
- Adequate number of GPIO pins
- ADC with multiple channels and good resolution (8-10 bits).
- Large programmable flash.

Keeping these requirements in mind, a short survey was conducted to compare and contrast different Bluetooth MCUs provided by popular manufacturers. The results of this survey are shown in Table 5.9.

CC2640 is selected because of the following reasons:

- Bluetooth 5 & 4.2 with Native SDK, examples and reference designs.
- Dedicated low power core for sensor polling.
- 8 channel ADC with 12 bit resolution and up-to 31 GPIOs.
- Low Power operation (1.8-3.8 V) with very low standby current (0.94 μA)
- Better development resources and inexpensive development kit.
- Support for Over The Air (OTA) firmware update.

5.8 Summary

Based on the global requirements and component specific requirements, different sensors, communication protocols and MCUs were compared. Following points summarise the hardware design decisions.

- Sensor characterization is performed for pressure and temperature sensors.
- Since simple resistor divider circuits does not meet any design requirements, new conditioning circuit are designed for pressure and temperature sensor.
- Use of conditioning circuit provides better accuracy, linearity and output range.
- Different wireless communication protocols are compared as they provide several advantages over wired communication protocols. Bluetooth is selected as preferred wireless communication protocol.
- Several Bluetooth MCUs are compared on basis of different parameters.
- Final sock design will feature following hardware components:
 - TekScan A301 FSR sensor to measure force/pressure.
 - Semitec 103JT NTC thermistor for temperature measurement.
 - MMA8451 Accelerometer to aid static/dynamic pressure measurements
 - TI CC2640R2F Bluetooth chip for sensor polling and communication.

Parameters	CC2642R	CC2640	BLUENRG-248	ATSAMB11XR/ZR
Manufacturer	TI	TI	ST	Microchip
Bluetooth Version	5.0	4.2	5.0	5.0
Other Protocols	UART,SSI,I2C,I2S	UART,SSI,I2C,I2S	UART, I2C,SPI	UART, SPI, I2C
GPIO	31	10/14/15/31	14/15/26/27	
ADC channels / resolution(bits)	8/12	8/12	NA/10	4/11
Programmable Flash	352KB	128KB	256KB	256KB
Clock	48-MHz	Up to 48-MHz	16/32 MHz	26 MHz
Crypto-engines	AEC/ECC/RSA/SHA2			AES-128,SHA-256
Voltage range	1.8 V to 3.8 V	1.8 V to 3.8 V	1.7 to 3.6V	2.3 - 4.3 V
Active mode RX	6.9 mA	5.9 mA		5.26 mA
Active mode Tx	9.6 mA (5dBm)	9.1 mA (5dBm)	10.9 mA (4dBm)	4.18 mA (peak)
Active mode MCU	3.4 mA	3.4 mA	3.3 mA	-
Standby	0.94 μ A	1 μ A	1 μ A	2.03 μ A
Cost (single)	5.49 <i>euro</i>	4.09 <i>euro</i>	3.14 <i>euro</i>	7.11 <i>euro</i>
Development-Kit cost	39.99 <i>USD</i>	29.99 <i>USD</i>	61.31 <i>euro</i>	-
Compliance	EN 300, 328 (Europe) and other	ETSI EN 300, 328 (Europe), EN 300 440 Class 2 (Europe)		
Other specifics	Low power sensor controller for sampling, buffering and processing analog and digital sensor data. Battery and temp monitor.			

Table 5.9: Comparison of different Bluetooth enabled microcontrollers

6 Software Design Exploration

Previous chapter provided information about design decisions leading to hardware selection and calibration of selected sensors. This chapter looks into design of Bluetooth firmware running on CC2640R2F Bluetooth MCU, and Android application that compliment hardware design.

6.1 Brief overview of Bluetooth Low Energy

Bluetooth Low Energy (BLE) is a low power wireless communication technology which utilizes the 2.4 GHz ISM band and targets battery powered devices. Bluetooth Core Specification Version 5.1 allows for two systems of wireless technology: Basic Rate (BR: BR/EDR for Basic Rate/Enhanced Data Rate) and Bluetooth Low Energy. The Bluetooth Low Energy system is designed to transmit small packets of data, while consuming significantly less power than BR/EDR devices.

Bluetooth LE offers several advantages such as low power operation, low cost modules and great market penetration of the BLE services. However low data rate, limited range and necessity of gateway to connect to internet can be seen as the limitation of the technology (Mohammad Afaneh, 2016).

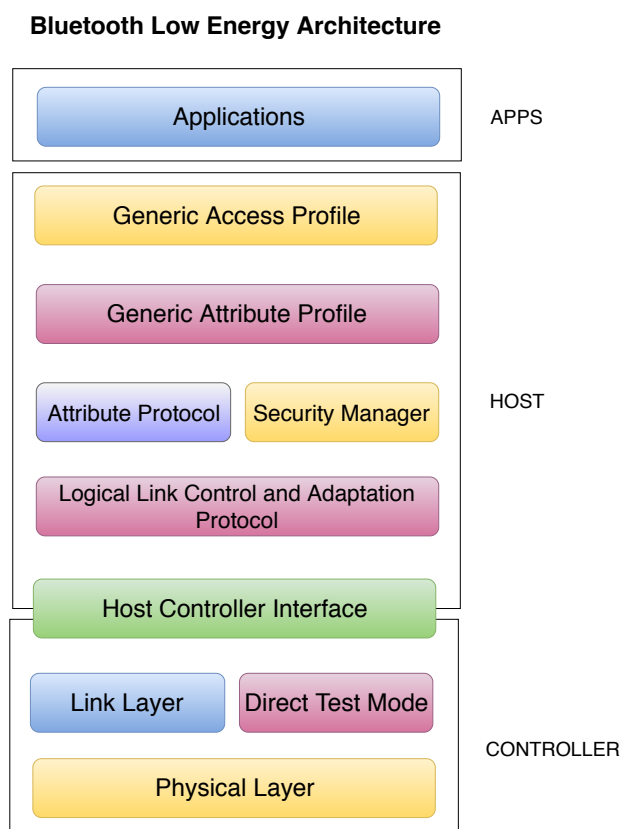


Figure 6.1: Bluetooth Low Energy Architecture. (Adopted from Mohammad Afaneh (2016))

Typical architecture of Bluetooth is shown in Figure 6.1. The Bluetooth architecture consists of different layers and these layers are grouped together according to the functionality. Usually Bluetooth chip manufacturers provide SDKs which completely take care of layers below Security Manager so that developers can focus on few defining layers such as GAP and GATT layer of the protocol. To define the sock firmware, these GAP and GATT profiles need to be defined.

Brief description of these profiles is given below:

Generic Access Profile (GAP)

Generic Access Profile is a basic framework that allows different devices to discover each other, establish connections, broadcast data and establish security services. This framework must be followed by every Bluetooth capable device and forms the foundation for Bluetooth services.

GAP defines several roles that device can assume. These roles are as follows:

- **Central:** Central role refers to link-layer master. Central role device is the one who listens to advertisement packets of other devices, initiates connection and allows devices to join the network. Due to asymmetry in link layer roles, connection initiation (central device's task) requires more computational energy than peripheral device and hence such role is given to devices with better CPU and memory resources (smartphones, computers etc).
- **Peripheral:** Peripheral refers to link-layer slave. Peripheral device start advertising to make Central device aware of its existence. Since peripheral role requires less complexity, its power and resource requirements are low, making this role more suitable for sensor nodes.
- **Observer:** Observers only listen to data contained in the broadcast packets from interested devices. Observer do not advertise or initiate connections. Their role can be seen similar to link-layer scanners.
- **Broadcaster:** Broadcaster devices broadcast data into their advertisement packets. This data can be sensor readings or other information. Broadcaster does not accept or initiate any connection requests.

It is important to note that GAP roles depend on context of communication and single device can operate in different roles simultaneously in different connections.

Generic Attribute Profile - GATT

Generic Attribute Profile (GATT) exposes services and format of the services offered by the end device. It also provides information about the procedures to access this data Mohammad Afaneh (2016). GATT uses Attribute Protocol defined in Bluetooth standard as its base protocol for transferring the data. According to this, the data is organized hierarchically into Services, characteristics and descriptors as shown in Figure 6.2.

This organization of GATT protocol is explained as follows:

- **Attribute** defines generic structure of data and it is used to describe any type of data exposed by GATT service. In fact, services and characteristics are also type of attribute.
- **Services** Services are relevant attributes (and characteristics) grouped on the basis of functionality. For example location service can contain different characteristics providing precise location information. Conceptually Services can be seen similar to class in object oriented language with each data variable as characteristics.
- **Characteristics** Characteristics are the data containers which provide piece of information about services exposed to the client. Characteristics is always a part of some service and can not exists on its own. Client Characteristic Descriptors (CCCD) also allow client to subscribe for updates in characteristic values.
- **Profiles** Profiles are broader in definition as compared to services and characteristics. Profiles define behaviour of client and server, services, connections and even security

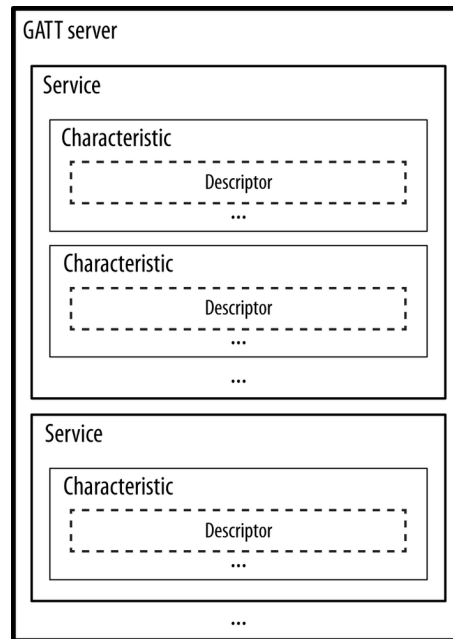


Figure 6.2: GATT protocol organization.

requirements. Profiles can be interpreted similar to application in Object Oriented language which utilizes different classes (services) along with other things to define complete behaviour.

The GAP and GATT profiles jointly describe the data exchange and connection characteristics of the Bluetooth devices. With this knowledge in our hand, we will now look into design of firmware running on smart-socks end device and android application that is used to log the parameter data.

6.2 CC2640 MCU Firmware

After understanding basics of Bluetooth in previous section, this section provides information about the Bluetooth MCU (CC2640R2F) and provides broad overview of the firmware design flow.

The CC2640R2F is a wireless micro-controller (MCU) targeting Bluetooth 4.2[®] and Bluetooth 5[®] low-energy applications. It contains a 32-bit ARM[®] Cortex[®]-M3 core that runs at 48 MHz as the main processor and a rich peripheral feature set which includes ultra-low power sensor controller. The sensor controller is ideal for interfacing external sensors and for collecting analog and digital data autonomously while the rest of the system is in sleep mode. CC2640R2F also has RF Core that offloads BLE service handling from main CPU. Bluetooth low energy controller and host libraries are embedded in ROM and run partly on this core. This architecture improves overall system performance and reduces power consumption. This also frees up significant amount of flash memory allowing more space for application.

Sock firmware is developed to take advantage of this three core structure of the MCU. Firmware is developed around the Software Development Kit(SDK Version 3.20) and examples provided by Texas Instruments for CC2640R2F BLE design. Sensor Controller Studio (version 2.4.0) is used for programming the sensor controller core and Code Composer Studio (version 9.1.0) is used to develop, debug and compile complete source code of the MCU.

Firmware developed for the sock is aimed to fulfill following characteristics:

- Continuous auto-updates of parameter values are sent to end device.

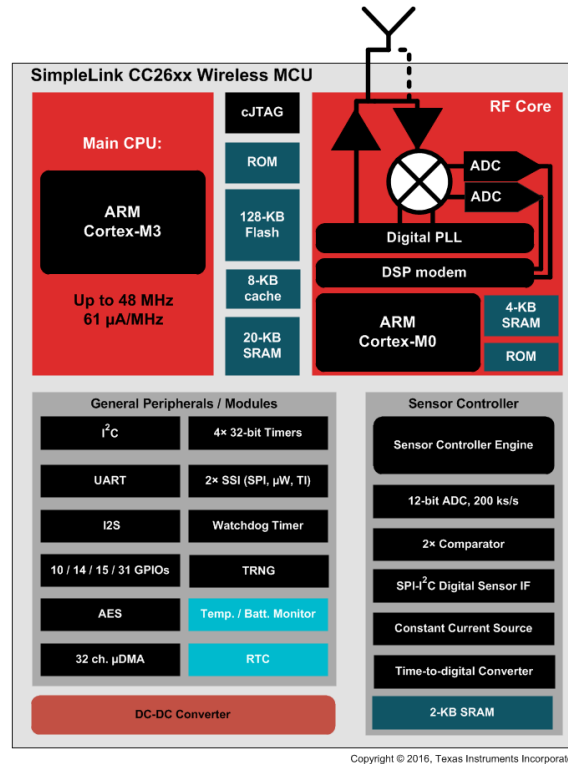


Figure 6.3: Functional block diagram of CC2640. (Image source: Texas Instruments)

- Sensor controller is used to poll sensors for reducing power consumption.
- Different sampling frequency is used for temperature and pressure sensors.

The brief firmware execution flow providing top level view of firmware design is explained below:

Firmware Execution Flow

Figure 6.4 provides brief overview of the firmware design. Each step of the firmware flow is explained in short as follows:

1. Upon power up hardware initialization is performed. This includes GPIO and board initialization, ADC initialization and I2C initialization. (UART initialization is performed if UART-debug is enabled).
2. Sensor Controller is initialized and its clock frequency is set to custom defined value. Sensor controller tasks (ADC sampling task and I2C task) are also initialized.
3. Bluetooth GAP and GATT services are initialized and registered.
4. Controller then starts advertising Bluetooth data. Advertisement is done indefinitely until either connection request is received or controller is turned off.
5. Upon connection, sensor controller tasks are enable which starts sampling of pressure and temperature readings as well as accelerometer data.
6. Sensor Controller samples the parameter data, alerts the main core for completion of sampling and schedules next task execution.
7. These readings are processed based on parameter type and an update is sent to the android application.

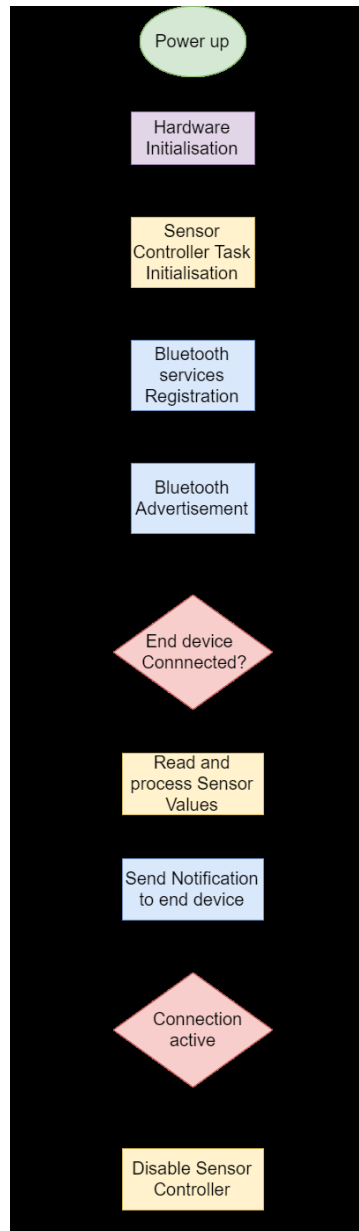


Figure 6.4: Execution flow of CC2640 firmware.

8. Data sampling and updating the end device continues until connection is terminated.
9. Upon connection termination, sensor controller tasks are disabled and controller goes back to advertisement state.

As explained earlier, Bluetooth has GAP profile for advertisement and different GATT profiles exposed to the end user for data transfer. These profiles have to be customised based on the application and the services provided by application. This is done based on firmware and end device requirements. For example, android BLE implementation allows maximum 20 bytes to be transferred per packet, so each parameter service is designed to fit within this data limit.

Figure 6.5 shows code snippets of different Bluetooth declarations. Figure 6.5a shows advertisement data structure, Figure 6.5b shows declaration of different characteristics and their respective UUID. Figure 6.5c shows structure of attribute Table which is used to expose all the parameter services to end user and Figure 6.5d gives example of how temperature parameter value is updated and notification update is attempted.

```

// GAP - Advertisement data (max size = 31 bytes, though this is
// best kept short to conserve power while advertising)
static uint8_t advertData[] = {
    0x02, // length of this data
    GAP_ADTYPE_FLAGS,
    DEFAULT_DISCOVERABLE_MODE | GAP_ADTYPE_FLAGS_BREDR_NOT_SUPPORTED,

    // complete name
    12,
    GAP_ADTYPE_LOCAL_NAME_COMPLETE,
    'S', 'm', 'a', 'r', 'k', 'e', 't', 't', 'i', 'n', 'g', ' ', 'S', 'o', 'c', 'k', 's',
};

```

(a) Bluetooth advertisement data

```

// Service UUID
#define SOCK_PARAMS_SERVICE_SERV_UUID 0x2BB2

// Characteristic definition
#define SOCK_PARAMS_SERVICE_PRESSURE_ID 0
#define SOCK_PARAMS_SERVICE_PRESSURE_UUID 0xC0A1
#define SOCK_PARAMS_SERVICE_PRESSURE_LEN 14

// Characteristic definition
#define SOCK_PARAMS_SERVICE_ACCELEROMETER_ID 1
#define SOCK_PARAMS_SERVICE_ACCELEROMETER_UUID 0xC0A2
#define SOCK_PARAMS_SERVICE_ACCELEROMETER_LEN 8

// Characteristic definition
#define SOCK_PARAMS_SERVICE_HEARTRATE_ID 2
#define SOCK_PARAMS_SERVICE_HEARTRATE_UUID 0xC0A3
#define SOCK_PARAMS_SERVICE_HEARTRATE_LEN 8

// Characteristic definition
#define SOCK_PARAMS_SERVICE_TEMP_ID 3
#define SOCK_PARAMS_SERVICE_TEMP_UUID 0xC0A4
#define SOCK_PARAMS_SERVICE_TEMP_LEN 12

```

(b) Bluetooth Sock Services Unique Identifiers (UUID)

```

static gattAttribute_t sock_params_serviceAttrTbl[] = {
    // sock_params_service Service Declaration
    { { ATT_BT_UUID_SIZE, primaryServiceUUID },
      GATT_PERMIT_READ,
      0, (uint8_t *) &sock_params_serviceDecl },
    // Press_temp Characteristic Declaration
    { { ATT_BT_UUID_SIZE, characterUUID },
      GATT_PERMIT_READ,
      0, &sock_params_service_Pressure_Props },
    // Press_temp Characteristic Value
    { { ATT_UUID_SIZE, sock_params_service_Pressure_UUID },
      GATT_PERMIT_READ,
      0, sock_params_service_Pressure_Val },
    // Press_temp CCCD
    { { ATT_BT_UUID_SIZE, clientCharCfgUUID },
      GATT_PERMIT_READ | GATT_PERMIT_WRITE,
      0, (uint8_t *) &sock_params_service_Pressure_Config },
    // Accelerometer Characteristic Declaration
    { { ATT_BT_UUID_SIZE, characterUUID },
      GATT_PERMIT_READ,
      0, &sock_params_service_AccelerometerProps },
    // Accelerometer Characteristic Value
    { { ATT_UUID_SIZE, sock_params_service_AccelerometerUUID },
      GATT_PERMIT_READ,
      0, sock_params_service_AccelerometerVal },
    // Accelerometer CCCD
    { { ATT_BT_UUID_SIZE, clientCharCfgUUID },
      GATT_PERMIT_READ | GATT_PERMIT_WRITE,
      0, (uint8_t *) &sock_params_service_AccelerometerConfig },

```

(c) Service attribute Table defining all available services

```

case SOCK_PARAMS_SERVICE_TEMP_ID:
    if (len <= SOCK_PARAMS_SERVICE_TEMP_LEN)
    {
        // copy data
        memcpy(sock_params_service_Temp_Val, value, len);
        Log_info2("SetParameter : %s len: %d", (IArg) "Temperature",
                (IArg) len);
        attrConfig = sock_params_service_Temp_Config;

        // Try to send notification.
        GATTServApp_ProcessCharCfg(
            sock_params_service_Temp_Config,
            (uint8_t *) &sock_params_service_Temp_Val, FALSE,
            sock_params_serviceAttrTbl,
            GATT_NUM_ATTRS(sock_params_serviceAttrTbl),
            ss_icall_rsp_task_id, sock_params_service_ReadAttrCB);
    }
    else
    {
        ret = bleInvalidRange;
    }
    break;

```

(d) Sending notification for parameter update

Figure 6.5: Selected code snippets of CC2640R2F firmware.

6.3 Android Application

The android application development is carried out keeping two goals in mind: data logging and data visualization. Android is chosen as end-device application platform since it offers ease of connection, portability, ease of operation and mobility. Keeping this in mind, an app called 'smart-socks' is developed which is customized for temperature, pressure, accelerometer data acquisition.

Application Characteristics

Development of the android app is carried out to fulfill following characteristics:

- The application only shows devices running smart-sock for ease of access.
- On connection, application registers itself for automatic parameter updates from the sock.
- Real time timestamped data logs are created and stored in '.csv' (comma separated values) format for each data logging activity.

- Different threads for data logging and GUI.
- Files can be found in separate folder called "Smart Socks" in internal storage.
- Data readings obtained from different parts of the foot are displayed in tabular form on the device screen.
- For better visualization, pressure and temperature readings can be illustrated on the foot outline at respective data acquisition position on device screen.
- Works on devices with android version > 6.0 (Marshmallow)

Design flow

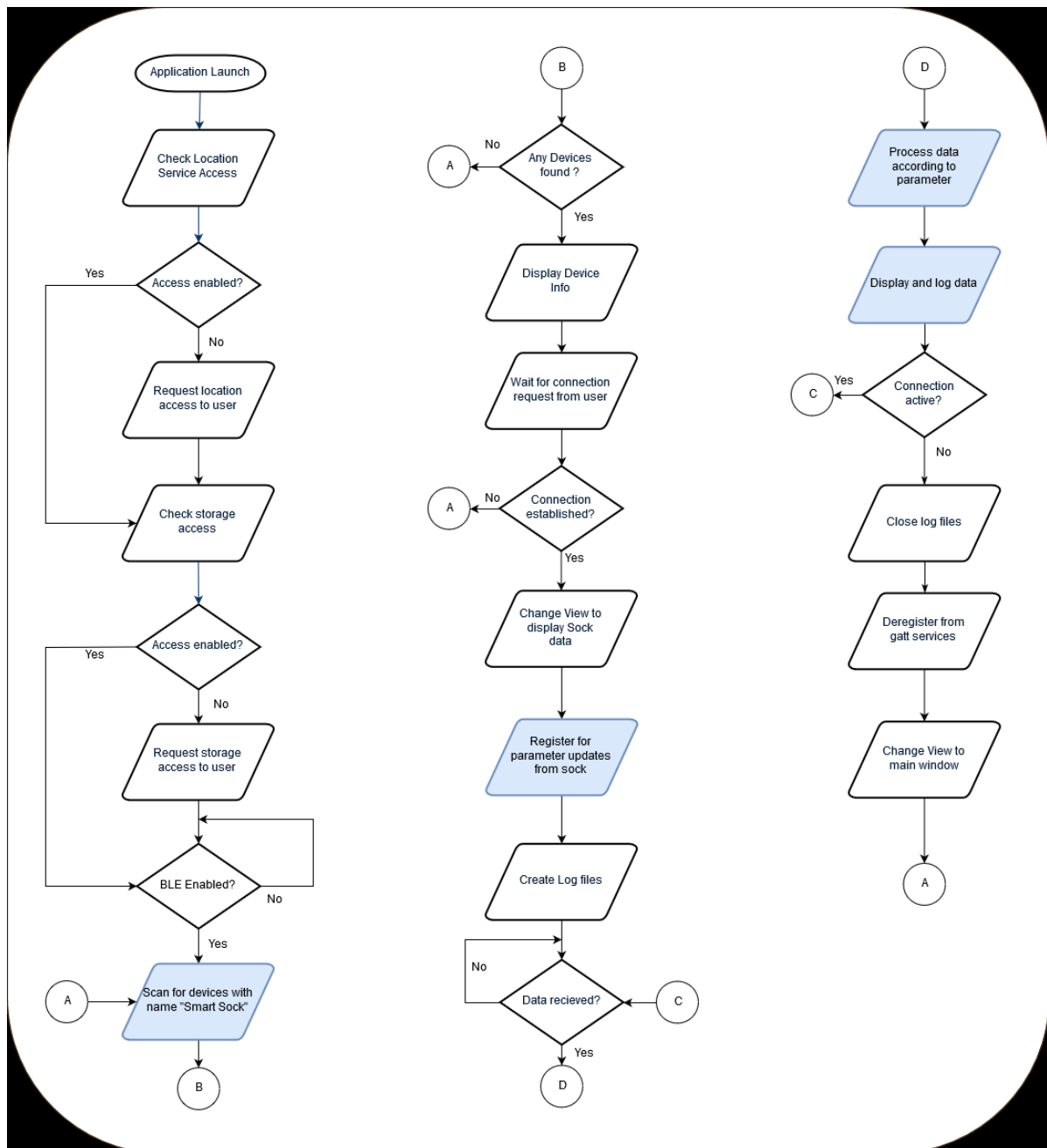


Figure 6.6: Abstract flow diagram of smart sock android application

Android app is developed using Android Studio IDE (version 3.5.1) with target android version 6.0 (Marshmallow) and above. As per the information on Android Studio, this application can work on almost 63% devices based on OS version. Figure 6.6 provides abstract version of application flow. Brief description of the application is as follows:

1. On application launch, access rights for location are requested from user as location is required to discover Bluetooth devices as per android guidelines.
2. Access to storage services is requested as it is required for creating and storing log files.
3. If any of these rights are not available, user is asked for these permissions as shown in Figure 6.7a.
4. If Bluetooth is on, device search is initiated. Application shows current Bluetooth status and buttons for turning Bluetooth on and off.
5. Only devices that match tag "Smart Socks" are displayed on the screen as shown in Figure 6.7b.
6. Connection is initiated on user request. Registration for automatic update of all parameter services is performed at the time of connection.
7. Application screen is changed for visualizing parameters as shown in Figure 6.7c.
8. New log files are created for temperature, pressure and accelerometer readings with naming format "SockData_MMddyyyyHHmmss_PARAMETER_NAME.csv" as shown in Figure 6.7d.
9. Upon reception of each packet, parameter service responsible for this data packet is resolved and data packet is processed accordingly.
10. Data is queued for logging and also displayed on the app screen.
11. In case user requests to terminate logging or connection is lost, log files are closed and application returns to device-search state.

This application has following design limitations:

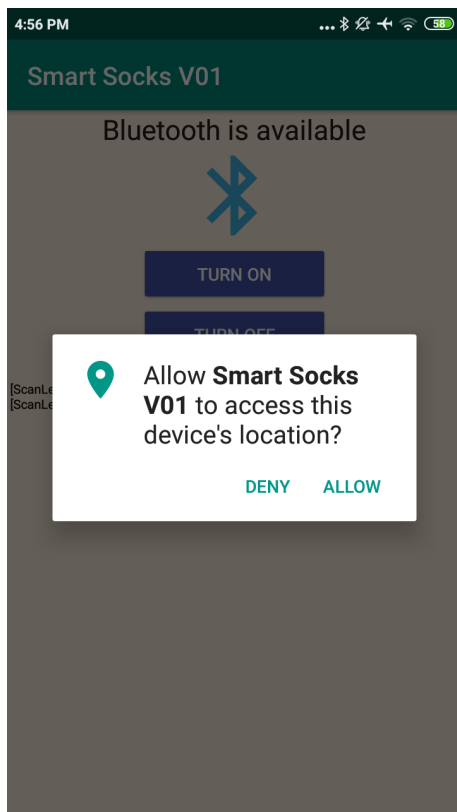
1. Bluetooth connection is terminated on change in orientation.
2. Bluetooth connection is terminated if application goes out of focus or phone is locked.
3. User has to explicitly turn on the Bluetooth service.

However these limitations do not pose any problem in data logging and can be overcome by simply enabling orientation lock and setting screen off time to zero.

6.4 Summary

- Bluetooth GAP and GATT services define Bluetooth end-devices behaviour.
- Separate services for temperature, pressure and accelerometer are defined and exposed to end user for gathering parameter values.
- These services also allow subscription to auto-updates in parameter values by using Client Characteristics Descriptor (CCCD) defined in Bluetooth protocol.
- Sock parameters are polled using low power sensor controller core which leads to reduction in power consumption.

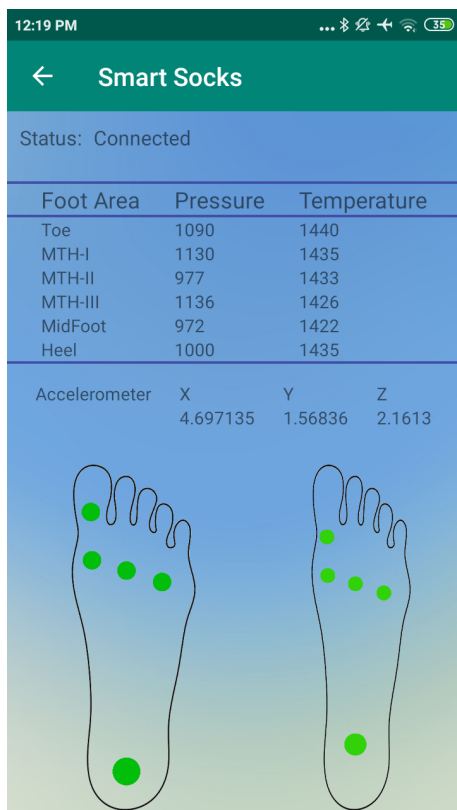
- Android application is developed for data logging as it provides ease of use, ease of connection and mobility.
- Data visualization can be also performed in the android application.
- Separate logs are generated for temperature, pressure and accelerometer.



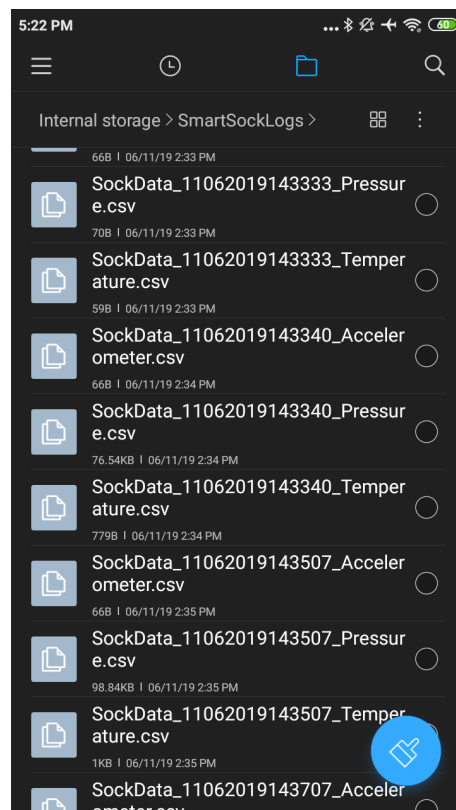
(a) Android App permissions



(b) Smart-Sock device discovery



(c) Data logging and visualization



(d) Generated log files

Figure 6.7: Examples of Android application screens.

7 System Integration

Chapter 5 and Chapter 6, provided design decisions for hardware and software components followed by characterization of sensor technologies and overview of firmware and android app design.

Once these components are individually characterized and tested, a prototype of working sock was developed integrating these components.

7.1 Sensor Placement

Sensor placement is important to maximize the effectiveness of the system. This section describes different locations for sensor placement and the reasoning behind selection of sensor placement positions.

Pressure and Temperature Sensor placement

Plantar foot area can be divided into 15 areas based on the foot pressure distribution as shown in Figure 7.1. These areas can be grouped into different regions such as heel (points 1-3), mid-foot (points 4-5), metatarsal (points 6-10), and toe (points 11-15). These regions support most of the body weight and experience majority of pressure changes. The measured force at these positions can be used to derive physiological, structural, and functional information of the lower limbs and whole body (Shu et al., 2010). Hence, it is very natural to select the sensor position from these location.

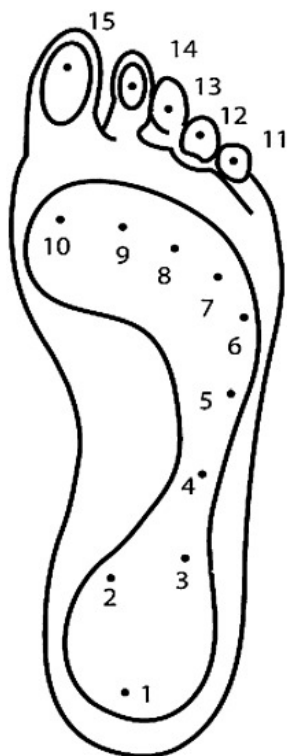


Figure 7.1: Different areas of the foot based on pressure distribution. (Adopted from (Shu et al., 2010))

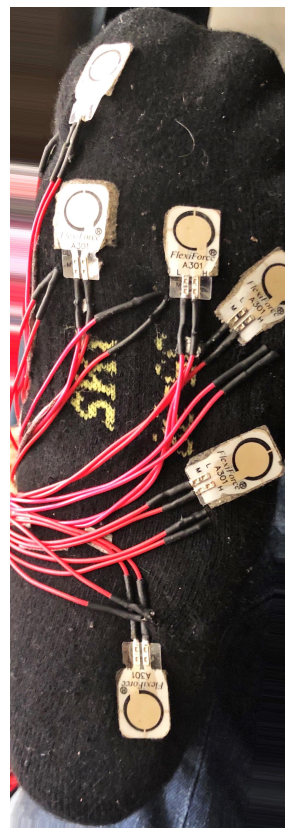


Figure 7.2: Pressure sensor locations on the plantar side of the foot. Temperature sensors are placed at the same location from the inside.

To reduce complexity of the sock design, only 6 locations were chosen to measure the pressure. To cover all the foot regions, sensors are distributed throughout the areas as follows: One sensor at the great toe (point 15), three sensors covering metatarsals (points 10, 8 & 6), one sensor at midfoot (point 4) and one sensor at heel (point 1). This sensor distribution on sock is shown in Figure 7.2. As explained by (Shu et al., 2010), many sport gadgets as well as clinical equipments use between 3-7 sensors for pressure measurements hence use of 6 pressure sensor is adequate for targeted clinical analysis.

Since temperature measurements are to be performed at locations where skin is exposed to high pressure and skin abrasion, temperature sensors are placed at the same location as pressure sensors. Only difference being, temperature sensors are placed inside the sock such that sensing unit will be directly in contact with the skin to get more accurate results. Lastly even though current design uses only 6 sensors, current hardware design supports up to 8 pressure and temperature sensors without any hardware modification.

Accelerometer Placement

Accelerometer is added to the sock to aid abnormal pressure detection as well as gait cycle detection. Bare abnormal pressure change can not be used to predict ulceration as it might be because of particular posture or movement of the leg. Accelerometer and pressure readings can be used to correlate the posture or movement of the foot and respective pressure distribution. The accelerometer is placed just above the heel, aligned with ankle line. This allows to detect the motion of complete foot as well as motion from the ankle joint.

7.2 Sock Version 1.0

Once sensor placement locations are decided, first working prototype is assembled and tested. This prototype uses custom designed PCB for signal conditioning. The integration steps for first prototype are explained in this section.

Sensor Breakout-board

For first version of the sock, a decision is made to use the CC2640R2F launchpad as the base board for sensor integration and RF communication. However, signal conditioning is required before sensor outputs can be given to ADC to sample the data. Moreover, there are only 8 ADC channels available at the controller whereas total number of sensors to be sampled range between 12-16. Hence, analog multiplexer should be used to multiplex these sensors to available ADC channels. A two-layer sensor breakout board is designed to facilitate the signal conditioning and multiplexing. This board is shown in Figure 7.3.

Complete Setup

Once this board is ready, complete setup is assembled and shown in Figure 7.4.

Limitations

- Use of two board design (Launchpad + Sensor Breakout Board) causes sock to be bulky making it uncomfortable to wear.
- This design also introduces additional connections from sensor board to controller.
- MCU Launchpad also includes additional peripherals and components that are not required for the desired application increasing size of the MCU circuit.
- Pressure sensors are directly exposed to the sock-shoe interface causing abrasion of sensor surface area.
- Current design uses small USB-power bank for powering the circuit.

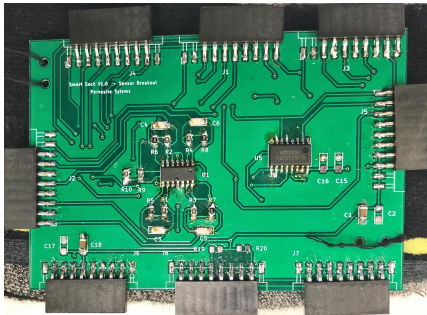


Figure 7.3: Sensor breakout board designed for sensor conditioning and multiplexing.



Figure 7.4: Sock prototype version-1

7.3 Sock Version 2.0

First prototype of sock design provided required functionality of the system however it had several limitation that prohibited its use in practical scenarios. All of these issues are addressed in the revised version. These issues are addressed by modifying the design as follows:

- Previous two board design was uncomfortable to wear, for this reason single PCB is designed which includes signal conditioning, micro-controller as well as RF circuitry.
- This design removes external conditioning circuit to controller connections making it relatively simple as compared to earlier design.
- Conductive thread is used to connect sensors to the PCB, which removes external cables that might cause hindrance for movement.
- The circuit is designed to work on coin cell battery removing dependency on external power source.
- This reduction in external cables also makes the sock more aesthetically pleasing as compared to earlier design.

Complete Setup

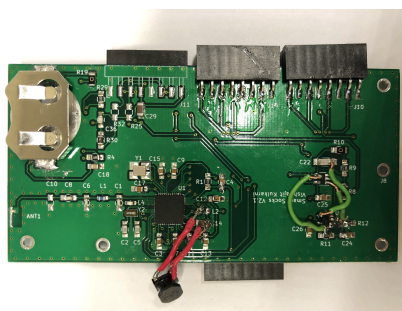


Figure 7.5: Single board design for signal conditioning, MCU and RF circuitry operated on coin-use of coin cell battery

Figure 7.6: Sock prototype version-2. Note the use of conductive thread removes dangling wire connections from the sensor.

Figure 7.5 illustrates the single board design including coin-cell holder for powering the device. Final assembled sock using designed board as well as conductive thread for sensor connections is shown in Figure 7.6.

7.4 Technical Difficulties

There were multiple technical difficulties encountered in the process of sock development. These difficulties are briefly described below:

- Heart-Rate sensor produced unreliable results due to even slightest movement of the foot. This movement hinders the working principal of the sensor hence idea of including heart rate sensor could not be realised.
- FSR data sheet recommends using piston like setup to exert known force values on the sensor. Such setup was not available for the sensor calibration. To address this issue, two versions of 3D printed test-jig were developed to distribute known weight over the desired area of the sensor and calibration was performed.
- Similar to FSR, temperature calibration requires known and stable temperature setup like environmental chamber. However, such setup was not available. It was addressed by using a setup where reference temperature of water was determined using a digital thermometer. The calibration of the sensor was then performed by comparing against this reference temperature.
- Determining the antenna path length for impedance matching was another challenge. This was mainly because of the difference in components size used on the launchpad and the ones used in the final version PCB, wherein, documentation was only available for the launchpad antenna settings.
- Single PCB design (final version of PCB) had ground loop issues which were difficult to single out and address.

7.5 Summary

- Once all sensors are characterised, system level integration is performed to assemble complete sock setup.
- Pressure and temperature sensors are positioned at different areas to cover foot areas experiencing most of the foot pressure.
- First version is based on CC2640R1F Launchpad + sensor breakout board.
- This version presents limitations such as dependency on external power source, wiring issues resulting in uncomfortable design.
- These issues are addressed as mentioned below:
 - Single board design for RF + microcontroller + signal conditioning.
 - Use of conductive thread for sensor connections
 - Coin-cell battery based operation

Both of these designs are evaluated based on different tests. These tests and obtained results will be discussed in next chapter.

8 Test and Evaluation

In this chapter, the different tests performed on the developed prototype of the smart sock are discussed and evaluated. Two versions of the sock have been developed. For each version, the following tests are performed where sensors were polled at 10Hz frequency.

- Pressure and Accelerometer Test
- Temperature Test

In addition to these tests, shoe evaluation test is also performed and discussed.

8.1 Sock Version 1 Test

In this section, the results of the tests performed on version 1 of the smart sock are presented and discussed.

8.1.1 Pressure Test and Accelerometer Test

Different Foot Postures

Once sock is ready, a simple test to assess functioning of pressure sensors was performed. For this, leg with the sock was kept in different position for around 20 seconds each. These postures are:

1. Standing still
2. Pressure on Heel
3. Pressure on Toe
4. Foot in the air

The result obtained for this test is shown in Figure 8.1 and Figure 8.2 below.

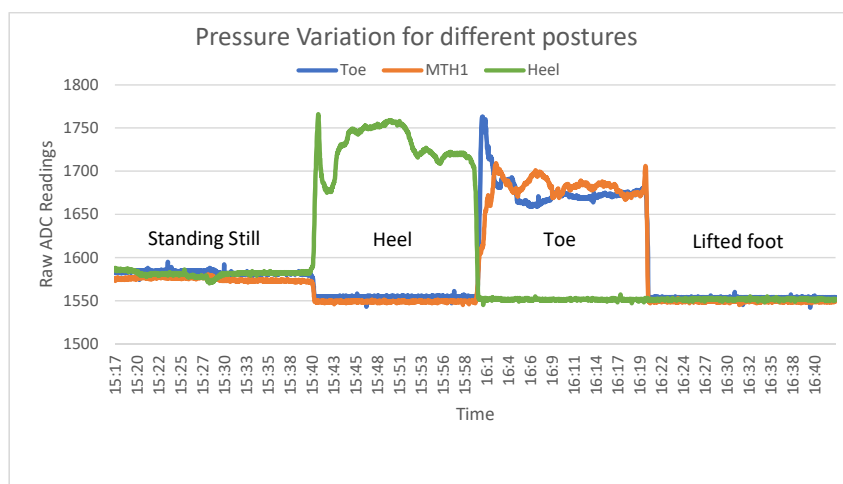


Figure 8.1: Variation in pressure readings at toe, MTH1 and heel for different postures. For all sensor readings refer Appendix C

As we can see, for standing still, almost all of the sensors show similar pressure indicating similar pressure distribution. When all of the pressure is put on heel by lifting toe up, FSR at heel position (green line in Figure 8.1) shows high pressure readings where as toe sensors show no

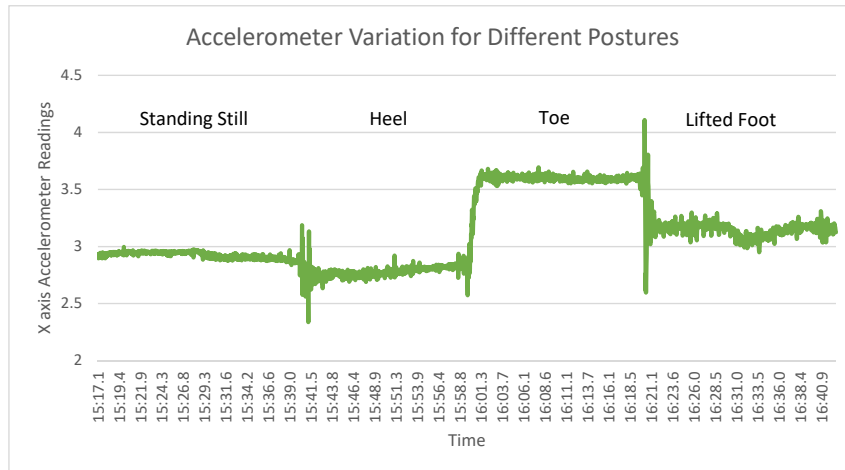


Figure 8.2: Variation in accelerometer readings for X axis for different postures.

load reading (op-amp reading for open circuit FSR).

Similarly when all body weight is put on toes by lifting heel side, pressure sensors located in top toe area (MTH-I, MTH-II), show high readings and pressure sensor near heel area show no load reading. Finally when foot is lifted completely and kept in the air, all the sensors give no-load reading confirming proper functioning of sensors.

Accelerometer readings are also analysed and result for x-axis change is shown in Figure 8.2. Since x-axis of the accelerometer was aligned with vertical movement of the foot, readings for x-axis are considered. Accelerometer is located in the back of the feet above the heel area. So its movement should correlate with heel movement. This behaviour can be confirmed from the plot as when the heel goes down accelerometer values decrease and when the heel goes up (while putting pressure on toe or floating foot state), accelerometer readings go high. This behaviour matches with expected behaviour from the accelerometer based on its positioning and alignment, demonstrating proper functioning of sensor.

Gait Analysis

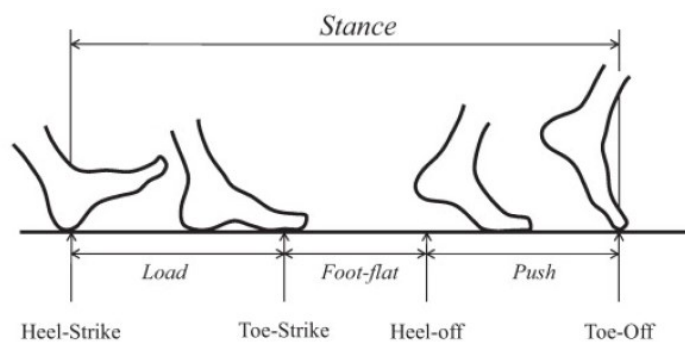


Figure 8.3: Different phases of gait cycle. (Adopted from (Mariani et al., 2013))

Once pressure and accelerometer readings were obtained for different postures, readings were taken for normal walking conditions to see variation in pressure of different foot areas as result of gait cycle. These changes in pressure values can be also used to isolate instances such as heel strike, toe strike, heel off, and toe off. This can be in turn used to check if pressure at these instances is within normal range and analyse overall gait characteristics of the patient. One such example of gait cycles recorded using pressure and accelerometer readings can be seen in Figure 8.4 and Figure 8.5.

The data was logged for 2 minutes and number of steps were recorded as well. For this particular test, total 53 steps with left leg (leg with smart-sock) were recorded. The results are shown in Figure 8.4. From this plot, following observations regarding gait can be made:

- As it can be observed, heel and toe pressure peak points are grouped together within short time spans.
- Heel pressure peak appears earlier than toe peak points which shows heel strike before toe.
- As heel is lifted up, pressure on toe will increase and hence we will get high toe pressure readings and no-load heel pressure reading. This is also evident in the plot.
- After toe lift (which indicates complete foot lift), and next heel strike, foot is in the air. This can be also confirmed as pressure values between peaks go to zero-load readings.
- Total peak count for any pressure sensor readings is 53, which is same as number of steps taken using leg under test. This further confirms effectiveness of this sensor arrangement for gait analysis.

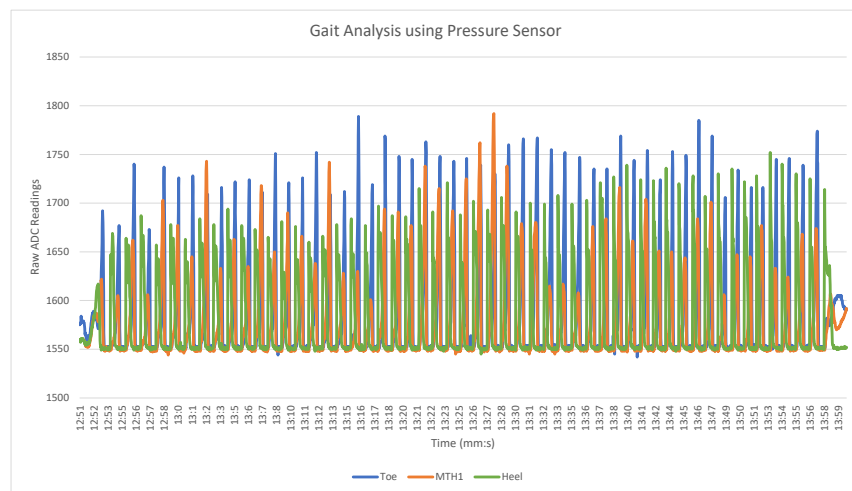


Figure 8.4: Pressure readings at toe, MTH1 and heel for gait cycle (53 steps each leg). For all sensor readings refer Appendix D

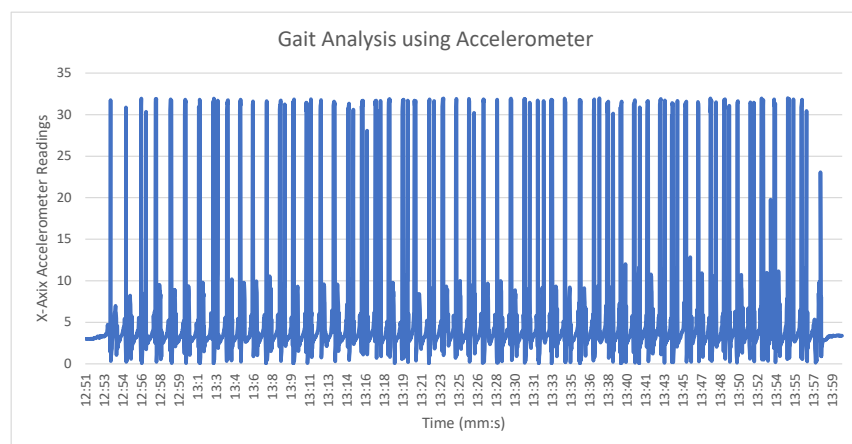


Figure 8.5: Accelerometer readings (x-direction) for gait cycle (53 steps each leg).

Similar to the earlier test, accelerometer readings were analysed for gait cycle as well. It can be also seen that that accelerometer readings (only x-direction readings are plotted here), show

distinct peaks as foot moves. These readings can be further used with pressure readings to confirm that pressure changes are indeed because of the movement of the foot and not due to abnormal changes or abnormal pressure distribution of the feet.

8.1.2 Temperature Test

Measuring foot temperature

Section 5.5.2 (Chapter 5) provided characterization results for temperature results. Obtained readings were accurate with just 1% error. In order to perform temperature profiling of the sock, a simple test with minimal foot movement is performed. The intention of this test is to check the response and stability of temperature readings when foot is not exposed to any temperature variation. The result of this test is shown in Figure 8.6. It can be seen from the plot that temperature readings are relatively constant conforming to the expected behaviour.

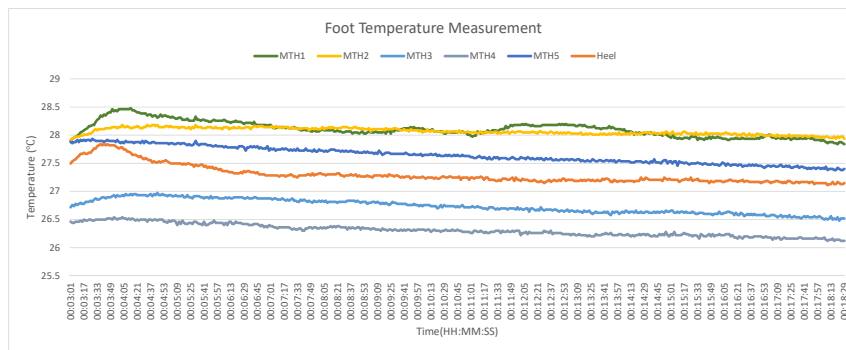


Figure 8.6: Temperature readings for different areas of the foot.

Measuring foot temperature variations

After normal foot temperature test yielded positive results, another test is performed to test how well the sock can responds to changes in temperature. To check this, foot is exposed to a heat source for few minutes and then taken away and placed in open air. To reflect such behaviour temperature readings should show increment for sometime and then shows decrement afterwards corresponding to the processes of exposing to and getting away from heat source. Plot of the temperature readings of this test are shown in Figure 8.7. Similar to earlier test this test also conforms to the expected behaviour.

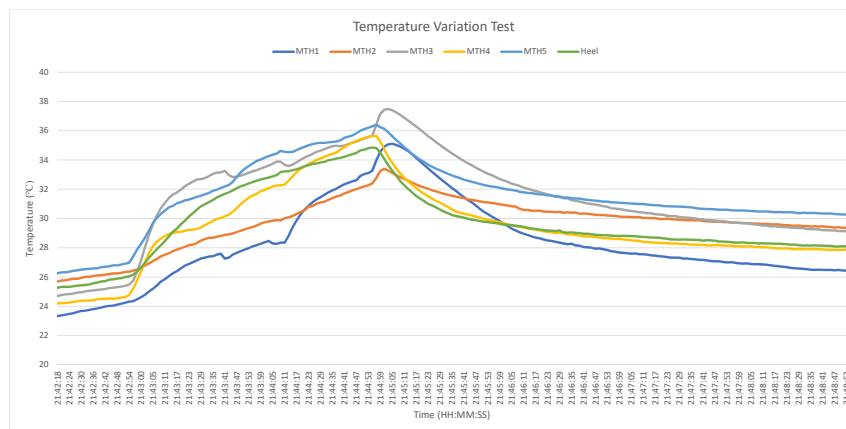


Figure 8.7: Temperature readings for different areas of the foot when foot is subjected to varying temperature using heat source.

Since maximum error in temperature readings is 0.2°C , maximum error in difference of temperature between left and right leg would be 0.4°C . This is within acceptable limit as we are interested in finding out difference of more than 2.2°C between same region of right and left foot.

8.2 Sock Version 2 Test

A revised prototype of the sock is designed to address the limitations and drawbacks observed in first prototype. This section describes the results of same set of tests performed on second version of the sock. Since most of the signal conditioning is kept same, it is expected to get similar characteristics as mentioned in previous section. The results of these tests are explained in this section.

8.2.1 Pressure and Accelerometer Test

8.2.2 Different Foot Postures

Pressure measurements for different foot postures are recorded in the similar way as described in previous section. Since basic conditioning circuit is same (except for reference voltage), it is expected to obtain similar graph.

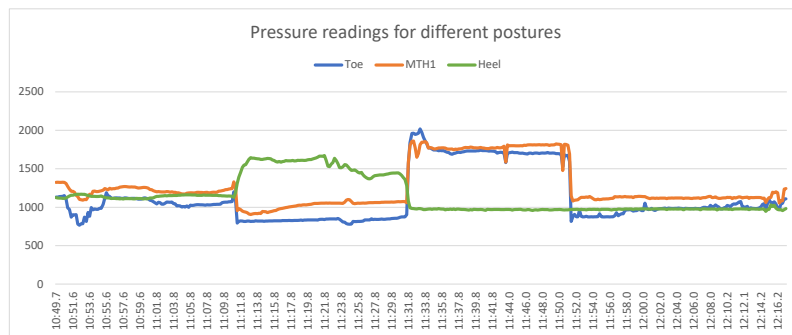


Figure 8.8: Pressure readings of Toe, MTH1 and heel for different postures.

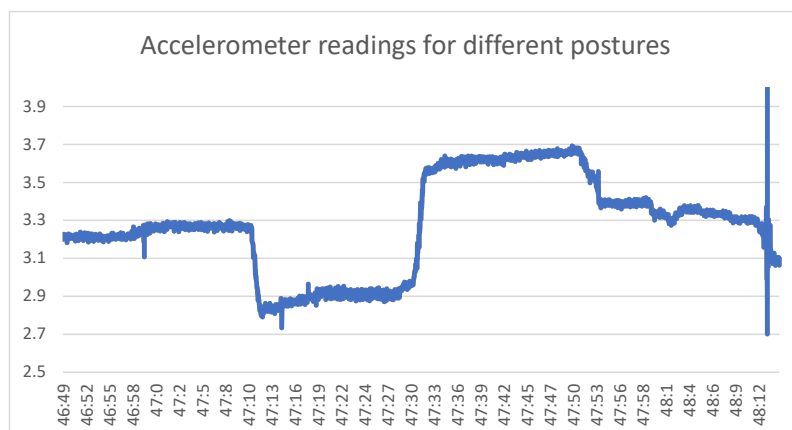


Figure 8.9: X-axis accelerometer readings for different postures.

8.2.3 Gait Analysis

Once the test for different foot posture is conducted, another test for gait analysis is conducted. For this test total of 19 foot steps are recorded with slow paced walking. Slow paced walking is

chosen to enhance the characteristics observed in gait analysis. Figure 8.10 and 8.11 show the obtained results for this test.

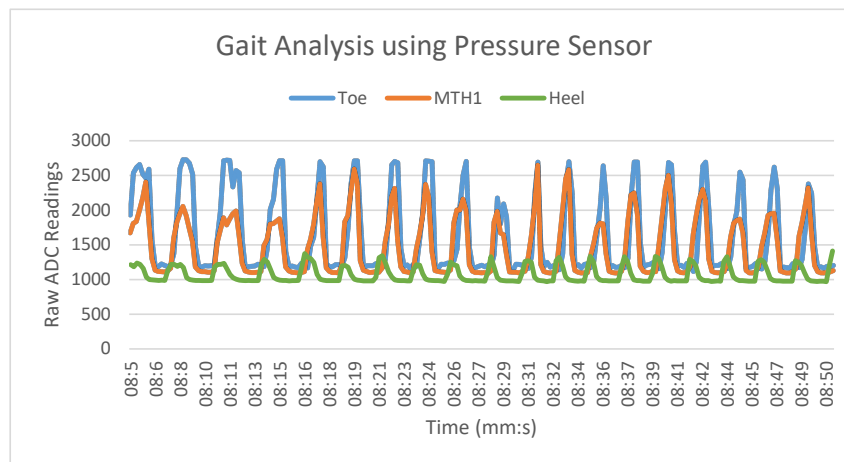


Figure 8.10: Pressure readings for gait cycle (19 steps each leg).

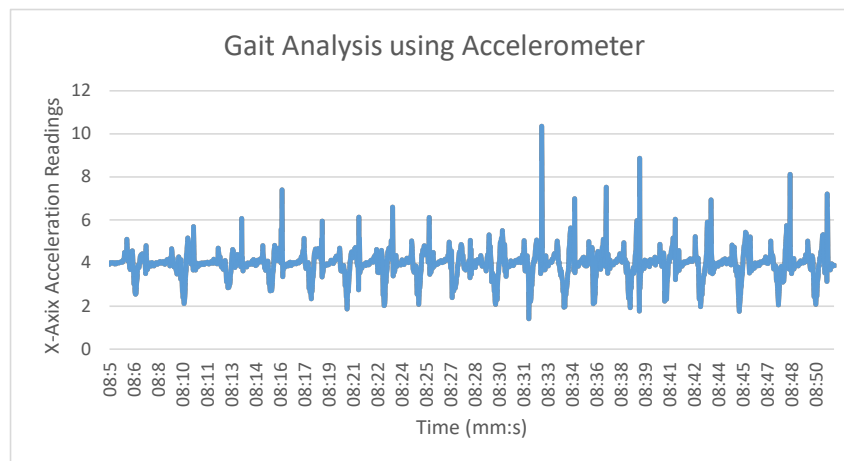


Figure 8.11: Accelerometer readings (x-direction) for gait cycle (19 steps each leg).

From Figure 8.10 following observations can be made:

- 19 distinct peaks pertaining to 19 steps can be observed in both the plots.
- In general toe area experiences more pressure as compared to heel while walking.
- Also heel strikes first and quickly goes off from the ground whereas toe remains in contact with the ground for longer duration.
- Pressure readings for both revised and earlier prototype show similar gait characteristics curves.

8.2.4 Temperature Test

Once pressure tests are performed, temperature tests are conducted in similar manner as described in previous section. Similar to previous methodology, two type of tests are performed to verify stability and response of the sensor. The response of the sock for these two tests are shown in Figure 8.12 and 8.13.

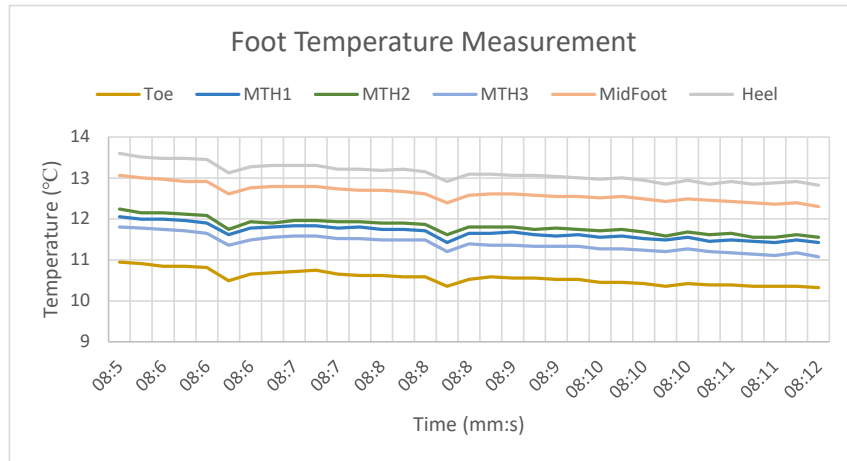


Figure 8.12: Temperature readings for different areas of the foot.

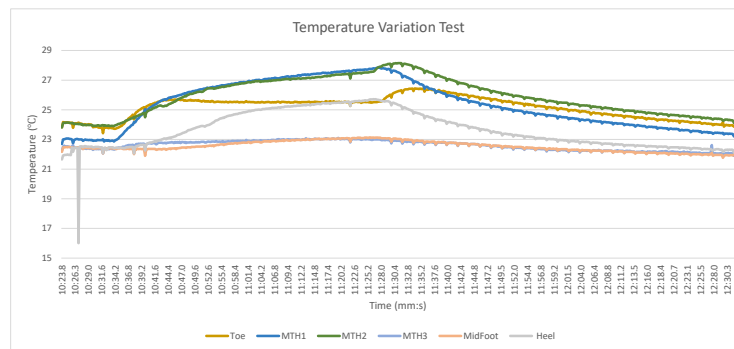


Figure 8.13: Temperature readings for different areas of the foot when foot is subjected to varying temperature using heat source.

Both graphs show behaviour similar to earlier test conducted for first version of the sock. This is expected as conditioning circuit used is same in both revisions.

8.3 Shoe Evaluation

Diabetic patients with high ulceration risk are advised to use custom footwear to offload the pressure from sensitive areas. This footwear is made by process similar to foot casting. However there is no definitive way to quantify the effectiveness of footwear. The sock designed for ulcer prediction can also be used for characterising the footwear.

A simple test is conducted to evaluate the use of sock for footwear performance. Pressure readings are obtained for two shoes worn by a female participant. The two shoes used for this test are shown in Figure 8.14. One shoe is typical sport shoe used for daily activities and other shoes is high-heel shoe. The test is conducted by putting both shoes one by one and recording readings for normal standing position. The result of this test is shown in Figure 8.15.

It is widely known that high-heel shoe is not good for back as well as foot since it creates uneven pressure distribution on the foot. This is clearly visible from the Figure 8.15. From Figure 8.15, toe and mid-foot area experiences increased pressure where as Meta-tarsal are (MTH I,II,III) observes reduced pressure when high-heels are worn. This indicates that this particular high-heel shoe forces foot to become arched between toe to mid-foot area causing unnatural distribution of pressure. Prolonged exposure to such abnormal pressure distribution can affect normal functioning of foot and back.



Figure 8.14: Different shoes (sport shoes and high-heel) used to evaluate their effectiveness in distribution of the foot pressure.

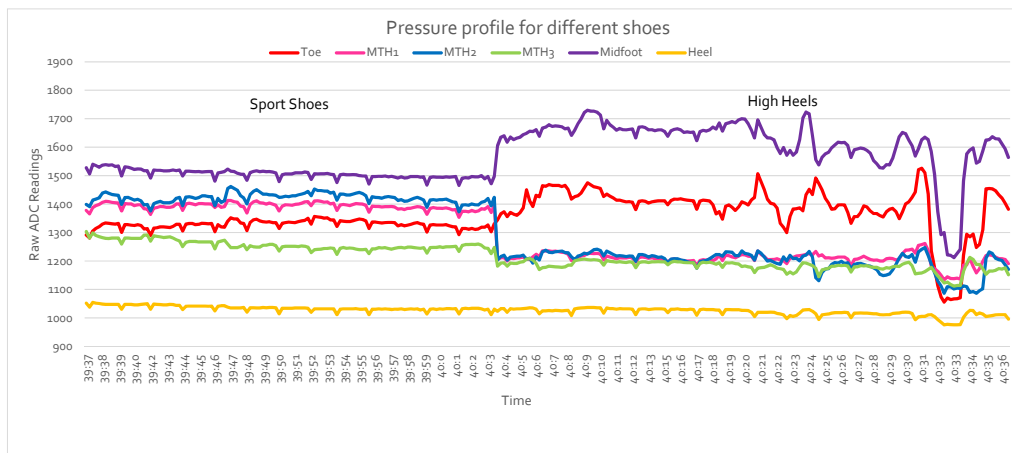


Figure 8.15: Pressure readings for sport shoes and high heels in standing position.

8.4 Power Profiling

Once all the system components are integrated and evaluated, power profiling of the final version of sock is performed to get better estimate of power consumption of the system.

For power analysis power analyser kit from Nordic Semiconductor is used. This kit provides power to the custom designed board connected as DUT (Device under test) and calculates average current measurement of the device. The test setup for current measurement is shown in Figure 8.16 and example of profiler test results for Bluetooth Advertising phase are shown in figure 8.17.

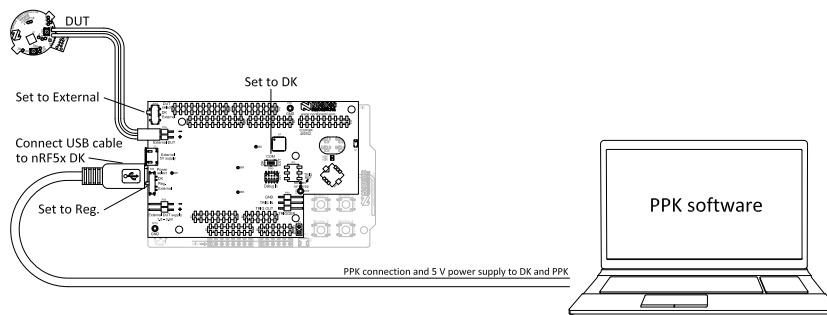


Figure 8.16: Test setup for power measurement. The Sock is connected as device under test (DUT).

To get better estimate of power consumption, three case scenarios are considered:

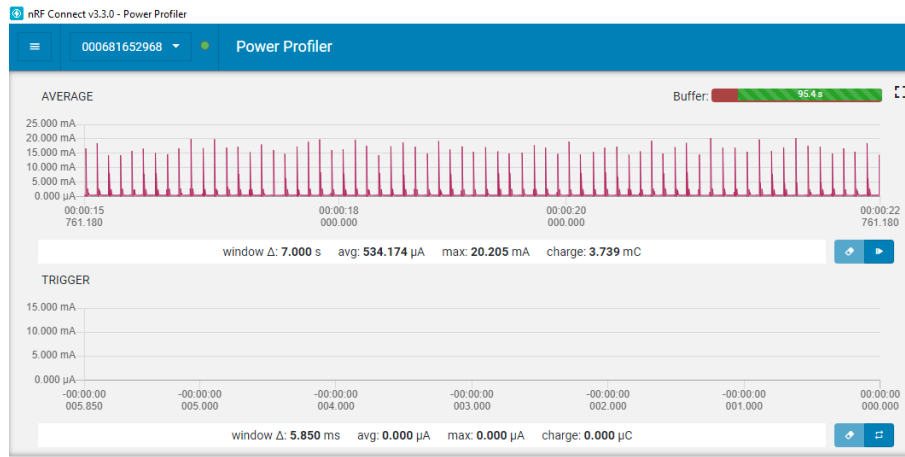


Figure 8.17: Power profiler results for Bluetooth advertising.

- Bluetooth advertising without any signal conditioning circuit
- Bluetooth Advertising + peripherals
- All Sensors polled at 10 Hz frequency

Average current consumption for continuous Bluetooth advertisement is $\approx 175\mu A$. However this figure goes up to $530\mu A$ as soon as additional signal conditioning circuitry is introduced along side the MCU. This is expected due to on current consumed by the sensors, op-amp and multiplexer circuits.

To avoid excess current consumption, controller is sent to stand-by mode when idle. Current consumption for active mode Bluetooth logging activity is around $2.75mA$. This is expected as sensor polling and Bluetooth transfer both takes place in this case.

As sock uses CR2032 coin cell battery which has capacity of 240mAH, sock will be functional for $240/2.75 = 87$ Hrs continuously. If a patient uses sock for 10 hours daily, this will give operating time of about 9 days.

Operating time of sock can be further improved using following measures:

- Optimized Bluetooth transfer by storing data locally and sending it over once in burst mode.
- Optimized hardware and PCB layout. Power consumption by MCU is also dependent on the RF circuitry and PCB layout. Current design uses 2 layer PCB which can result in ground path issues. This performance can be improved by using correct impedance matching circuit along with 4 layer design of the PCB.

With 10Hz sampling frequency, the difference between advertising and data transmission current is around 2.2 mA. This is the amount of current consumed for 10 samples of each foot parameter. Roughly speaking each sampling event of all parameters will consume around 0.22 mA. This clearly marks dependency of the overall current consumption on the sampling frequency. Since temperature changes are not substantially different, temperature sensor can be polled at very low frequency ranging near 1Hz or even below that. This will effectively result in less polling of 6 temperature sensors leading to reduced power consumption and effectively better battery life.

8.5 Usability and washability

Washability and usability are the practical parameters outlined in the non-functional requirements section. Since sock is developed to measure foot parameters of diabetic patients, it should be comfortable to wear and walk. To assess this, sock was provided to seven participants (three female, four male) and series of questions about the usability of the test were asked.

The feedback form provided following questions:

- How easy it is to wear the sock (score 1-5)?
- How comfortable is to have the sock on while sitting? (score 1-5)
- how comfortable is to walk with the sock with shoes on? (score 1-5)
- How comfortable is to walk with the sock without shoes? (score 1-5)
- Do you consider this a useful solution? (Y/N)
- What do you want to see changed in the design to use such a sock yourself?

The overall experience results are positive. The scores provided by all users is summarised in Table 8.1 and Figure 8.18.

Participant ID	Gender	ease of wearing	comfort (sitting)	comfort (walking without shoe)	comfort (walking with shoe)
1	M	4	4	4	4
2	F	3	4	4	4
3	F	3.5	4.5	4	4
4	M	3.5	4	4	4
5	M	3	4.5	5	4
6	M	4	2	2	3
7	F	4	4	4	4
Average	-	3.71	3.85	3.85	3.85

Table 8.1: Usability survey results

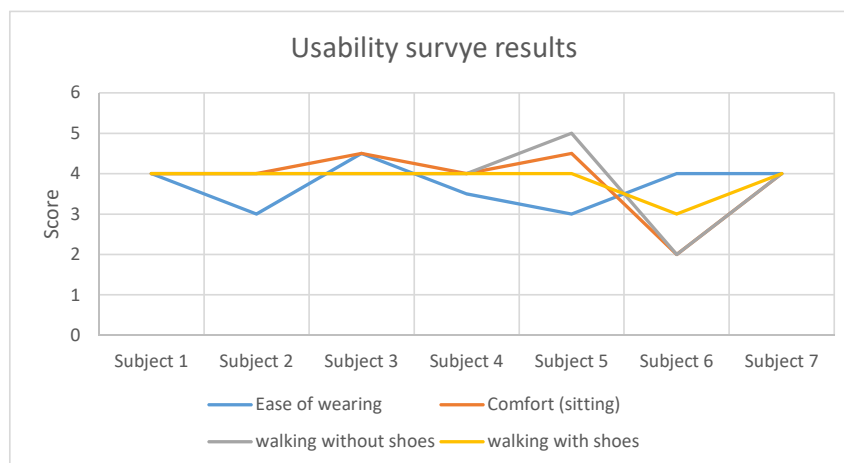


Figure 8.18: Summary of usability test results

Apart from this, users were asked to provide suggestions regarding improvement in the sock design. Following suggestions were received:

- Fabric layer to cover socks present on both inside and outside of the sock.
- Sensor integration into fabric.
- Reduction in PCB size.

In terms of design three suggestions were provided : padding near sensor connection area of the sock, reduction in PCB size, change in sensor connectors on the PCB.

Before washability test, a information available about sensor is used to predict washability results:

- Sock can not be used in washing machine or with detergents as it will affect sensor positions as well as behaviour hence simple dip test in the water must be performed.
- Temperature sensor readings were obtained by dipping it into the hot water, hence temperature sensor is expected to behave normally after the wash.
- Signal conditioning is designed such that any short between sensor terminals will result in saturation of op-amp output. This can be used as an indicator of the any short circuit due to water content in the sock.
- FSR and accelerometer must be tested physically and their response post wash must be recorded.
- Conductive thread might get shorted if there is water content available in the sock

After this sock (without the PCB) was dipped in the water and kept on heater for drying. On connecting sock back to the PCB and readings are observed. The sock did not produce in expected manner and produced erroneous results. This might be either due to damage to pressure sensors or short circuit on conductive fiber. Hence sock design can not be washed without any modification.

8.6 Summary

This chapter presented different evaluation tests and its results for temperature, pressure and accelerometer. Following points summarise the evaluation results:

- Different tests are performed for temperature and pressure tests.
- Different tests conducted are as follows:
 - Pressure sensor test for four different steady postures is conducted.
 - Gait analysis readings using pressure variation and accelerometer readings are also recorded.
 - Two temperature tests are performed to check temperature sensor behaviour.
- All of these tests confirm to expected behaviour proving suitability of the sock for desired purpose.
- A small test is performed to demonstrate use of the sock for shoe evaluation.
- Apart from this weight of the PCB is measured and found to be around 25 grams.
- Usability feedback has been recorded from two test subjects alongside prediction of washability test results.

- Once, the custom PCB is paired with the app continuous monitoring of foot parameters can be performed as long as power is available. A coin cell is used as the power supply for the sock. To determine the exact time for which the battery will last power analysis is done. Power analysis results conform to the requirement obtaining continuous data samples for long duration.
- A normal shoe and high-heel shoe pressure distribution is evaluated. It is observed that high-heel creates uneven pressure distribution making it unsuitable for long term use.

9 Conclusion

At the start of the thesis, a set of research question and sub questions were formulated to help in designing the smart-socks to monitor diabetic foot ulcer indicators. This chapter tries to provide answers to these research questions.

Which foot parameters can be used to predict incidence of diabetic foot ulcer?

An extensive literature survey was conducted to understand causes and effects of diabetes on normal functioning of the body. There is ample literature available that looks into which foot parameters can be monitored to predict ulceration of diabetic foot. These findings are summarised as below:

- Both static and dynamic pressure can be used to measure pressure distribution of the foot under different conditions.
- Foot area with consistent pressure greater than $6\text{kg}/\text{cm}^2$ ($\approx 600\text{kPa}$) is considered as site with risk of ulceration.
- Forefoot to rearfoot ratio (F/R) value of 2 or more can also be used to predict ulceration.
- Persistent temperature difference of 2.2°C or more between one region of the foot and same region on the contralateral foot is an strong indicator for ulceration.
- Persistent temperature changes can be observed upto one week before ulceration.
- Use of pH change as indicator of ulceration lacks sufficient support from literature to be considered as primary indicator. However it can be used as secondary parameter or additional information to gain better insights.
- In addition to this, degree of foot perfusion indicating state of blood supply of the foot is also an important and neglected parameter. Heart-rate can be used to check foot perfusion.

What are functional and non-functional requirements of monitoring these parameters using a smart sock

At the start of the thesis following functional and non-functional requirements were outlined for sock. These requirements are as follows:

Functional Requirements

1. The developed sock should be able to monitor required foot parameters continuously.
2. Sock should be designed to be worn in day to day life. Design should be clean and should not affect or change the normal bio-mechanics of the foot causing errors in the readings.
3. Sensors data must be reproducible and repeatable
4. Sufficient battery life must be ensured to take continuous readings for long duration.
5. Errors in sensor readings must be within specified limits.
6. System should be able to perform data logging.

Non-functional Requirements

1. *Safety*: The sock is designed for patients with neuropathy, which means they have very little or no sensation of pain. Thus it should be made sure that, the sock is not causing any damage to the foot skin while attempting to measure the same.
2. *Weight*: Weight of the sock should not cause any effect on walking or foot health.
3. *Sock design* should be size independent.
4. *Sock* should be washable and reusable within certain restrictions.

What are the software and hardware requirements and design decisions for continuous monitoring and detection of foot ulcer using a smart sock?

Complete design of sock to monitor these foot parameters is divided into three different parts: sock hardware, sock firmware and android application for data logging. To design the complete system, different design decisions were made as explained in Chapter 5 and 6. These design decisions are summarised below:

- Force sensing resistors are used to measure force/pressure observed by different areas of the foot.
- Accelerometer is added to aid static and dynamic pressure measurements. Addition of accelerometer also enables the system to perform gait analysis as described in Chapter 8.
- NTC thermistors were used to monitor temperature of the foot.
- Bluetooth MCU with dedicated core for sensor polling is selected to reduce power consumption of the device.
- Conditioning circuit is designed for temperature and pressure sensors to provide better accuracy and linear response. Sensor characterization and calibration is also performed.
- pH sensors and Heart-Rate sensors are not used due to design limitations.
- Android application is designed to visualize and log all parameter values.
- Coin cell operated custom printed circuit board is designed and evaluated.

How accurately and efficiently the designed smart sock can measure the foot ulcer indicators?

For both versions of the sock, performance is evaluated using different tests.

- Sock design is aimed to gather continuous parameter data for long duration of time.
- Pressure and temperature sensors were calibrated to meet accuracy requirement. For example, sock targets to measure temperature difference of 2°C or more, whereas designed sock provides accuracy of 0.15°C thereby meeting design requirement.
- Multiple readings are taken and analysed for the sensors to evaluate stability of the readings.
- Accelerometer is added to aid the correct interpretation of acquired pressure sensor readings.
- Sock tests are also conducted on two additional subject to confirm the desired performance of the sock.

How user-friendly and comfortable is the designed smart sock?

To determine the usability of the sock, tests were performed using two subjects. In addition to this, users were asked series of questions regarding the usability and comfort of the sock design. Feedback from both users provided overall positive experience such as intuitive app design among others mentioned previously. Few suggestions for improvement were also provided which can be seen as future scope of the research.

After answering all sub-questions outlined at the start of the research, this thesis concludes by addressing the main research question.

To what extent, is it possible to continuously monitor foot ulcer indicators in an efficient, accurate, and user- friendly manner through embedding sensing and communication technologies in daily worn socks?

From the literature survey, it is clear that strong indicators are present which can be monitored for predicting ulceration. Proposed sock is designed such that it can be worn throughout the day at home as well as outside. This design aims to achieve more monitoring time than shoe or insole based systems. Since sock design is powered using coin cell, it can work independently. Use of Bluetooth and android application facilitate data collection and make the overall sock design easy to use. Hence, this design can provide more data samples leading to better prediction of diabetic foot ulcer.

Having said that, this sock design is still in preliminary stage and many avenues are available for improvement in both design and functionality of the sock. These prospects will be discussed in the following chapter.

10 Future Work

This chapter provides few ideas about the possible improvements and additions to the current sock design.

1. **Energy Harvesting:** The current sock design uses a lithium ion coin cell to power the complete circuit. However there are systems are available which make use of the movement of the foot itself (among other techniques) to harvest energy and power themselves. Such energy harvesting can also be integrated with the current sock design to completely eliminate the battery usage or reduce the dependency on it.
2. **Use of Smart Materials:** The sock design in this thesis uses external sensors placed on a sock. Instead of using sensors placed externally, special materials which are capable of determining pressure and temperature values can be used.
3. In addition to use of smart materials for pressure and temperature sensing, flexible PCBs or fabric printed PCBs can be used.
4. Currently Android app monitors the data only from one foot. By taking advantage of the Bluetooth mesh in Bluetooth 5.0, a single application could be deployed to monitor data from both the legs simultaneously.
5. A neural network can be trained to analyse the received sensor data on the end-point device to provide real time evaluation of the foot.

Bibliography

- Ahmad, J. (2016), The diabetic foot, **vol. 10**, no.1, pp. 48 – 60, ISSN 1871-4021, doi:<https://doi.org/10.1016/j.dsx.2015.04.002>.
<http://www.sciencedirect.com/science/article/pii/S1871402115000302>
- Al-Sarawi, S., M. Anbar, K. Alieyan and M. Alzubaidi (2017), Internet of Things (IoT) communication protocols, in *2017 8th International conference on information technology (ICIT)*, IEEE, pp. 685–690.
- Alavi, A., R. G. Sibbald, D. Mayer, L. Goodman, M. Botros, D. G. Armstrong, K. Woo, T. Boeni, E. A. Ayello and R. S. Kirsner (2014), Diabetic foot ulcers: Part I. Pathophysiology and prevention, **vol. 70**, no.1, pp. 1–e1.
- Ali, S. M. and G. Yosipovitch (2013), Skin pH: from basic science to basic skin care, **vol. 93**, no.3, pp. 261–269.
- Armstrong, D. G., K. Holtz-Neiderer, C. Wendel, M. J. Mohler, H. R. Kimbriel and L. A. Lavery (2007), Skin temperature monitoring reduces the risk for diabetic foot ulceration in high-risk patients, **vol. 120**, no.12, pp. 1042–1046.
- Association, A. D. et al. (2013), Diagnosis and classification of diabetes mellitus, **vol. 36**, no.Supplement 1, pp. S67–S74, ISSN 0149-5992.
http://care.diabetesjournals.org/content/36/Supplement_1/S67
- Association, A. D. et al. (2017), 2. Classification and diagnosis of diabetes, **vol. 40**, no.Supplement 1, pp. S11–S24.
- Bandyk, D. F. (2018), The diabetic foot: Pathophysiology, evaluation, and treatment, **vol. 31**, no.2, pp. 43 – 48, ISSN 0895-7967, doi:<https://doi.org/10.1053/j.semvascsurg.2019.02.001>, fighting Diabetic Foot Ulcers.
<http://www.sciencedirect.com/science/article/pii/S0895796719300110>
- Baynest, H. W. (2015), Classification, Pathophysiology, Diagnosis and Management of Diabetes Mellitus.
- Bernard, T., C. D’Elia, R. Kabadi and N. Wong (2009), An early detection system for foot ulceration in diabetic patients, in *2009 IEEE 35th Annual Northeast Bioengineering Conference*, IEEE, pp. 1–2.
- Bonnie C. Baker (2004), AN685:Thermistors in Single Supply Temperature Sensing Circuits.
<https://www.microchip.com/wwwAppNotes/AppNotes.aspx?appnote=en011704>
- Boulton, A. J., L. Vileikyte, G. Ragnarson-Tennvall and J. Apelqvist (2005), The global burden of diabetic foot disease, **vol. 366**, no.9498, pp. 1719 – 1724, ISSN 0140-6736, doi:[https://doi.org/10.1016/S0140-6736\(05\)67698-2](https://doi.org/10.1016/S0140-6736(05)67698-2).
<http://www.sciencedirect.com/science/article/pii/S0140673605676982>
- Caselli, A., H. Pham, J. M. Giurini, D. G. Armstrong and A. Veves (2002), The forefoot-to-rearfoot plantar pressure ratio is increased in severe diabetic neuropathy and can predict foot ulceration, **vol. 25**, no.6, pp. 1066–1071.
- Coates, J., A. Chipperfield and G. Clough (2016), Wearable multimodal skin sensing for the diabetic foot, **vol. 5**, no.3, p. 45.
- Duckworth, T., A. Boulton, R. Betts, C. Franks and J. Ward (1985), Plantar pressure measurements and the prevention of ulceration in the diabetic foot, **vol. 67**, no.1, pp. 79–85.

- Falanga, V. (2005), Wound healing and its impairment in the diabetic foot, **vol. 366**, no.9498, pp. 1736 – 1743, ISSN 0140-6736, doi:[https://doi.org/10.1016/S0140-6736\(05\)67700-8](https://doi.org/10.1016/S0140-6736(05)67700-8).
<http://www.sciencedirect.com/science/article/pii/S0140673605677008>
- Fierheller, M. and R. G. Sibbald (2010), A clinical investigation into the relationship between increased periwound skin temperature and local wound infection in patients with chronic leg ulcers, **vol. 23**, no.8, pp. 369–379.
- Frykberg, R. G., T. Zgonis, D. G. Armstrong, V. R. Driver, J. M. Giurini, S. R. Kravitz, A. S. Landsman, L. A. Lavery, J. C. Moore, J. M. Schuberth, D. K. Wukich, C. Andersen and J. V. Vanore (2006), Diabetic Foot Disorders: A Clinical Practice Guideline (2006 Revision), **vol. 45**, no.5, Supplement, pp. S1 – S66, ISSN 1067-2516, doi:[https://doi.org/10.1016/S1067-2516\(07\)60001-5](https://doi.org/10.1016/S1067-2516(07)60001-5), diabetic Foot Disorders: A Clinical Practice Guideline (2006 Revision).
<http://www.sciencedirect.com/science/article/pii/S1067251607600015>
- Gonçalves, C., A. Ferreira da Silva, J. Gomes and R. Simoes (2018), Wearable e-textile technologies: A review on sensors, actuators and control elements, **vol. 3**, no.1, p. 14.
- Healy, A., P. Burgess-Walker, R. Naemi and N. Chockalingam (2012), Repeatability of WalkinSense® in shoe pressure measurement system: A preliminary study, **vol. 22**, no.1, pp. 35–39.
- Hegde, N. and E. S. Sazonov (2015), SmartStep 2.0-A completely wireless, versatile insole monitoring system, in *2015 IEEE International Conference on Bioinformatics and Biomedicine (BIBM)*, IEEE, pp. 746–749.
- Jason Gums (2018), Types of Temperature Sensors.
<https://www.digikey.com/en/blog/types-of-temperature-sensors>
- Jeffcoate, W. J. and K. G. Harding (2003), Diabetic foot ulcers, **vol. 361**, no.9368, pp. 1545 – 1551, ISSN 0140-6736, doi:[https://doi.org/10.1016/S0140-6736\(03\)13169-8](https://doi.org/10.1016/S0140-6736(03)13169-8).
<http://www.sciencedirect.com/science/article/pii/S0140673603131698>
- John Maynard (2015), How Wounds Heal: The 4 Main Phases of Wound Healing.
<https://www.shieldhealthcare.com/community/wound/2015/12/18/how-wounds-heal-the-4-main-phases-of-wound-healing/>
- Jon Gabay (2013), Choosing an Amplifier/Conditioning Circuit to Interface with Thermocouples.
<https://www.digikey.com/en/articles/techzone/2013/apr/choosing-an-amplifierconditioning-circuit-to-interface-with-thermocouples>
- Jones, B. F. (1998), A reappraisal of the use of infrared thermal image analysis in medicine, **vol. 17**, no.6, pp. 1019–1027, ISSN 0278-0062, doi:10.1109/42.746635.
- Lambers, H., S. Piessens, A. Bloem, H. Pronk and P. Finkel (2006), Natural skin surface pH is on average below 5, which is beneficial for its resident flora, **vol. 28**, no.5, pp. 359–370.
- Lavery, L. A., D. G. Armstrong, R. P. Wunderlich, J. Tredwell and A. J. Boulton (2003), Predictive value of foot pressure assessment as part of a population-based diabetes disease management program, **vol. 26**, no.4, pp. 1069–1073.
- Lavery, L. A., K. R. Higgins, D. R. Lanctot, G. P. Constantinides, R. G. Zamorano, K. A. Athanasiou, D. G. Armstrong and C. M. Agrawal (2007), Preventing diabetic foot ulcer recurrence in high-risk patients: use of temperature monitoring as a self-assessment tool, **vol. 30**, no.1, pp. 14–20.

- Lepántalo, M., J. Apelqvist, C. Setacci, J.-B. Ricco, G. De Donato, F. Becker, H. Robert-Ebadi, P. Cao, H. Eckstein, P. De Rango et al. (2011), Chapter V: diabetic foot, *European Journal of Vascular and Endovascular Surgery*, **vol. 42**, pp. S60–S74.
- Levy, M. J. and J. Valabhji (2008), The diabetic foot, **vol. 26**, no.1, pp. 25–28.
- Lin, X. and B.-C. Seet (2016), Battery-free smart sock for abnormal relative plantar pressure monitoring, **vol. 11**, no.2, pp. 464–473.
- Lincoln, L. S., M. Quigley, B. Rohrer, C. Salisbury and J. Wheeler (2012), An optical 3D force sensor for biomedical devices, in *2012 4th IEEE RAS & EMBS International Conference on Biomedical Robotics and Biomechatronics (BioRob)*, IEEE, pp. 1500–1505.
- Liu, C., J. J. van Netten, J. G. Van Baal, S. A. Bus and F. van Der Heijden (2015), Automatic detection of diabetic foot complications with infrared thermography by asymmetric analysis, **vol. 20**, no.2, p. 026003.
- Liu, C., F. van der Heijden, M. Klein, J. van Baal, S. Bus and J. van Netten (2013), Infrared dermal thermography on diabetic feet soles to predict ulcerations: a case study, in *Advanced Biomedical and Clinical Diagnostic Systems XI*, Eds. A. Mahadevan-Jansen, T. Vo-Dinh and W. Grundfest, SPIE, Proceedings of SPIE, ISBN 978-0-8194-9417-7, doi:10.1117/12.2001807.
- Mariani, B., H. Rouhani, X. Crevoisier and K. Aminian (2013), Quantitative estimation of foot-flat and stance phase of gait using foot-worn inertial sensors, **vol. 37**, no.2, pp. 229 – 234, ISSN 0966-6362, doi:<https://doi.org/10.1016/j.gaitpost.2012.07.012>.
http:
[//www.sciencedirect.com/science/article/pii/S0966636212002822](http://www.sciencedirect.com/science/article/pii/S0966636212002822)
- Mohammad Afaneh (2016), The Basics of Bluetooth Low Energy (BLE).
<https://www.novelbits.io/basics-bluetooth-low-energy/>
- Mostafalu, P., A. Tamayol, R. Rahimi, M. Ochoa, A. Khalilpour, G. Kiaee, I. K. Yazdi, S. Bagherifard, M. R. Dokmeci, B. Ziaie et al. (2018), Smart bandage for monitoring and treatment of chronic wounds, **vol. 14**, no.33, p. 1703509.
- Najafi, B., H. Mohseni, G. S. Grewal, T. K. Talal, R. A. Menzies and D. G. Armstrong (2017), An optical-fiber-based smart textile (smart socks) to manage biomechanical risk factors associated with diabetic foot amputation, **vol. 11**, no.4, pp. 668–677.
- Ono, S., R. Imai, Y. Ida, D. Shibata, T. Komiya and H. Matsumura (2015), Increased wound pH as an indicator of local wound infection in second degree burns, **vol. 41**, no.4, pp. 820–824.
- Patrick Mannion (2017), Comparing Low Power Wireless Technologies.
<https://www.digikey.com/en/articles/techzone/2017/oct/comparing-low-power-wireless-technologies>
- Perrier, A., N. Vuillerme, V. Luboz, M. Bucki, F. Cannard, B. Diot, D. Colin, D. Rin, J.-P. Bourg and Y. Payan (2014), Smart Diabetic Socks: Embedded device for diabetic foot prevention, **vol. 35**, no.2, pp. 72 – 76, ISSN 1959-0318, doi:<https://doi.org/10.1016/j.irbm.2014.02.004>.
http:
[//www.sciencedirect.com/science/article/pii/S1959031814000220](http://www.sciencedirect.com/science/article/pii/S1959031814000220)
- Price, C., D. Parker and C. Nester (2016), Validity and repeatability of three in-shoe pressure measurement systems, *Gait & posture*, **vol. 46**, pp. 69–74.
- Razak, A., A. Hadi, A. Zayegh, R. K. Begg and Y. Wahab (2012), Foot plantar pressure measurement system: A review, **vol. 12**, no.7, pp. 9884–9912.
- Reiber, G., B. Lipsky and G. Gibbons (1998), The burden of diabetic foot ulcers, **vol. 176**, no.2, pp. 5S–10S.
- dos Reis, M. d. C., F. A. Soares, A. F. da Rocha, J. L. Carvalho and S. S. Rodrigues (2010), Insole with pressure control and tissue neoformation induction systems for diabetic foot, in *2010 Annual International Conference of the IEEE Engineering in Medicine and Biology*, IEEE, pp.

- 5748–5751.
- Reyzelman, A. M., K. Koelewyn, M. Murphy, X. Shen, E. Yu, R. Pillai, J. Fu, H. J. Scholten and R. Ma (2018), Continuous Temperature-Monitoring Socks for Home Use in Patients With Diabetes: Observational Study, **vol. 20**, no.12, p. e12460.
- Saito, M., K. Nakajima, C. Takano, Y. Ohta, C. Sugimoto, R. Ezoe, K. Sasaki, H. Hosaka, T. Ifukube, S. Ino et al. (2011), An in-shoe device to measure plantar pressure during daily human activity, **vol. 33**, no.5, pp. 638–645.
- Selvin, E., S. Marinopoulos, G. Berkenblit, T. Rami, F. L. Brancati, N. R. Powe and S. H. Golden (2004), Meta-analysis: glycosylated hemoglobin and cardiovascular disease in diabetes mellitus, **vol. 141**, no.6, pp. 421–431.
- Shu, L., T. Hua, Y. Wang, Q. Li, D. D. Feng and X. Tao (2010), In-Shoe Plantar Pressure Measurement and Analysis System Based on Fabric Pressure Sensing Array, **vol. 14**, no.3, pp. 767–775, doi:10.1109/TITB.2009.2038904.
- Tan, A. M., F. K. Fuss, Y. Weizman, Y. Woudstra and O. Troynikov (2015), Design of Low Cost Smart Insole for Real Time Measurement of Plantar Pressure, *Procedia Technology*, **vol. 20**, pp. 117 – 122, ISSN 2212-0173, doi:<https://doi.org/10.1016/j.protcy.2015.07.020>, proceedings of The 1st International Design Technology Conference, DESTTECH2015, Geelong.
<http://www.sciencedirect.com/science/article/pii/S2212017315001978>
- Tekscan (2019), How Does a Force Sensing Resistor (FSR) Work?
<https://www.tekscan.com/blog/flexiforce/how-does-force-sensing-resistor-fsr-work>
- Waaijman, R., M. de Haart, M. L. Arts, D. Wever, A. J. Verlouw, F. Nollet and S. A. Bus (2014), Risk factors for plantar foot ulcer recurrence in neuropathic diabetic patients, **vol. 37**, no.6, pp. 1697–1705.
- Zimmet, P., K. Alberti and J. Shaw (2001), Global and societal implications of the diabetes epidemic, **vol. 414**, no.6865, p. 782.

A Complete test results : Thermistor calibration using conditioning circuit

T_{ref}	No. of Samples	Raw ADC Reading	ADC (V)	$R_{calculated}$	$T_{calculated}$	Error ($^{\circ}C$)	Error (%)
25.1	22	1877.0909	1.98681	9903.452642	25.29601695	-0.19601695	0.780944042
25.9	18	1914.7778	2.026618	9614.976533	26.08255102	-0.18255102	0.704830196
26.7	21	1947.667	2.061968	9372.539174	26.76489999	-0.06489999	0.243071125
27.4	26	1988.8846	2.105252	9091.840039	27.58083384	-0.18083384	0.659977533
28.3	11	2034.4545	2.1541	8794.592062	28.47718052	-0.17718052	0.62607956
29.4	20	2101.65	2.224711	8397.716895	29.73003061	-0.33003061	1.122553086
30.3	18	2142.3889	2.268538	8168.908661	30.48381562	-0.18381562	0.606652225
31	13	2190.3846	2.318936	7920.739558	31.32946359	-0.32946359	1.062785775
31.5	23	2209.2609	2.338761	7827.201132	31.6561784	-0.1561784	0.495804444
32.3	22	2255.7272	2.388602	7601.518452	32.46339481	-0.16339481	0.505866292
32.5	30	2262.0333	2.395224	7572.509371	32.56916069	-0.06916069	0.21280212
33	16	2298.8125	2.433844	7407.641258	33.17929805	-0.17929805	0.543327429
33.8	18	2350.7222	2.4894	7182.682847	34.03763845	-0.23763845	0.70307235
34.8	14	2397.8579	2.538898	6993.461061	34.78406773	0.015932272	0.045782391
35.1	16	2423.8125	2.566154	6893.461913	35.18804043	-0.08804043	0.250827423
36.3	10	2504.8	2.652243	6595.580961	36.43282525	-0.13282525	0.36590979
36.7	19	2541.5263	2.691417	6468.391276	36.98431529	-0.28431529	0.774701069
37	24	2555.2917	2.706314	6421.301912	37.19168774	-0.19168774	0.518074967
37.8	32	2595.6875	2.74873	6290.904042	37.77525761	0.024742391	0.065456062
38.2	27	2623.4762	2.777913	6204.220853	38.17100323	0.02899677	0.075907774
38.6	13	2659.067	2.816345	6093.64457	38.68523649	-0.08523649	0.220819924
39.1	23	2693.2173	2.852194	5993.995057	39.15800993	-0.05800993	0.14836298
39.7	8	2747.75	2.908012	5845.164528	39.88135847	-0.18135847	0.456822337
40.2	24	2768.0417	2.931812	5783.929304	40.18520343	0.014796573	0.036807396
40.8	16	2826.9375	2.990507	5638.258113	40.92326916	-0.12326916	0.302130301
41.1	31	2849.2258	3.01774	5573.133594	41.26042503	-0.16042503	0.390328531
41.7	22	2892.9545	3.064032	5465.817427	41.82611237	-0.12611237	0.302427739
42.3	19	2945.9474	3.120008	5341.446044	42.49805835	-0.19805835	0.468223053
43.2	16	3014.1875	3.192382	5188.790633	43.34809597	-0.14809597	0.342814745
43.7	20	3062.4	3.243955	5085.227877	43.94148316	-0.24148316	0.552593055
44.5	14	3091.7143	3.274841	5025.162142	44.29211538	0.207884624	0.467156458

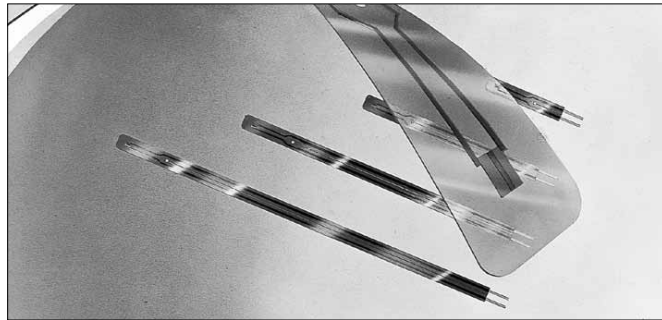
Table A.1: Complete test results for temperature sensor calibration using conditioning circuit.

B Datasheet: Temperature Sensor

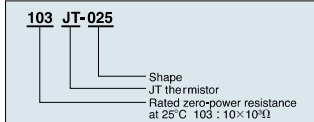
ULTIMATE THINNESS, JT THERMISTOR 500μm only

JT THERMISTOR

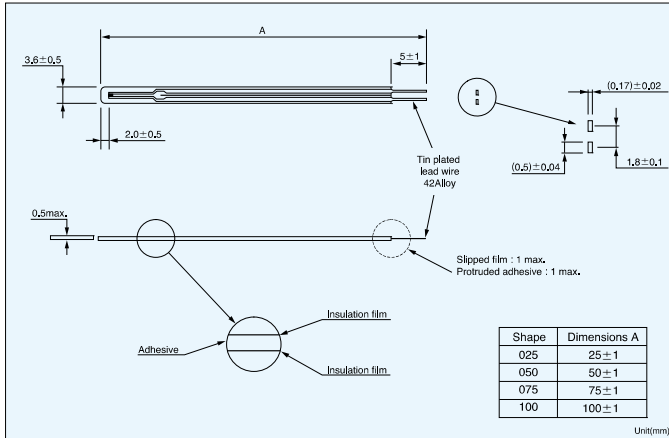
JT thermistors feature ultra thinness of 500μm and superior electrical insulation. It is possible to use with safety in ambience that might contact with electrodes.



Part number



Dimensions



Resistance-Temperature

Temperature (°C)	Type	
	103JT	104JT
-50	367.7	9584
-40	204.7	4572
-30	118.5	2282
-20	71.02	1191
-10	43.67	647.2
0	27.70	365.0
10	18.07	212.5
20	12.11	127.7
30	8.301	78.88
40	5.811	50.03
50	4.147	32.51
60	3.011	21.61
70	2.224	14.66
80	1.668	10.13
90	1.267	7.135
100	0.9753	5.111
110	0.7597	3.720
120	0.5981	2.746
125	0.5331	2.371

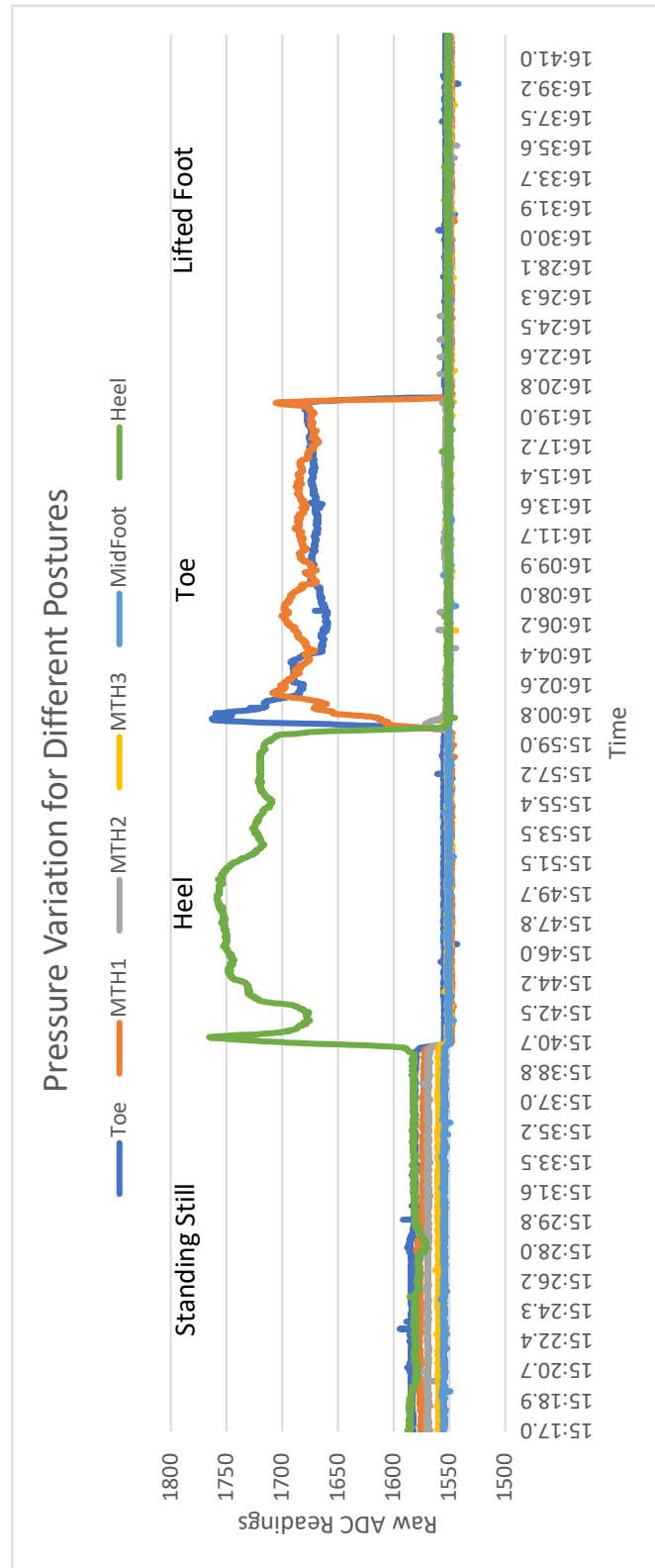
Unit:(kΩ)

Specifications

Part No.	R ₂₅ ^{*1}	B value ^{*2}	Dissipation factor (mW/°C) Approx.	Thermal time constant(s) ^{*3} Approx.	Rated maximum power dissipation(at 25°C)(mW)	Category temp. range(°C)
103JT-□□□	10kΩ ± 1%	3435K ± 1%	0.7	5	3.5	-50 ~ + 125
104JT-□□□	100kΩ ± 1%	4390K ± 1%				

*1 R₂₅ : Rated zero-power resistance value at 25°C, ±2% and 3% are also available.
 *2 B value : determined by rated zero-power resistance at 25°C and 85°C.
 *3 Time when thermistor temperature reaches 63.2% of the temperature difference. The value is measured in the air.

C Complete pressure sensor readings for different postures



D Complete pressure readings for gait analysis

